

ISSN 1023-9855



# 胸腔醫學

## Thoracic Medicine

The Official Journal of Taiwan Society of  
Pulmonary and Critical Care Medicine

Vol.32 No.6 December 2017

第三十二卷 第六期

中華民國一〇六年十二月



台灣胸腔暨重症加護醫學會

10048 台北市常德街 1 號

No. 1, Changde St., Jhongjheng Dist.,

Taipei City 10048, Taiwan



ISSN 1023-9855



Vol.32 No.6 December 2017

# 胸腔醫學

## Thoracic Medicine

The Official Journal of Taiwan Society  
of Pulmonary and Critical Care Medicine

### 原著

- 乙醯半胱氨酸在大白鼠模式下對酸吸入後伴隨呼吸器引發之急性肺損傷的作用 ..... 245~258  
鄭鴻志，陳奇祥，陳欽明

### 病例報告

- 肺部良性轉移性平滑肌瘤－病例報告與文獻回顧 ..... 259~265  
姜佑承，林旻希，賴瑞生
- 透過肺泡灌洗術診斷念珠菌肺炎－病例報告 ..... 266~271  
洪緯欣，陽光耀
- IgG4相關疾病以肋膜侵犯和呼吸喘表現 ..... 272~278  
林珮瑜，古世基
- Castleman氏病的支氣管內視鏡超音波影像－案例報告 ..... 279~285  
陳永瑄，何肇基
- 同時性原發性肺癌的特殊病理發現病例報告 ..... 286~290  
何蕙如，洪維亨，王秉彥



Vol.32 No.6 December 2017

# 胸腔醫學

## Thoracic Medicine

The Official Journal of Taiwan Society  
of Pulmonary and Critical Care Medicine

### Original Articles

- Effect of N-acetylcysteine on Acid Aspiration Followed by Ventilator-Induced Acute Lung Injury in a Rat Model.....245~258  
Hung-Tze Tay, Khee-Siang Chan, Chin-Ming Chen

### Case Reports

- Pulmonary Benign Metastasizing Leiomyoma: A Case Presentation and Review of the Literature .....259~265  
You-Cheng Jiang, Min-Hsi Lin, Ruay-Sheng Lai
- Candida* Pneumonia Diagnosed by Bronchoalveolar Lavage: A Case Report.....266~271  
Wei-Hsin Hung, Kuang-Yao Yang
- IgG4-Related Disease with Pleural Involvement Presenting as Progressive Dyspnea .....272~278  
Pei-Yu Lin, Shih-Chi Ku
- Endobronchial Ultrasound Imaging of Castleman's Disease: Two Case Reports .....279~285  
Yung-Hsuan Chen, Chao-Chi Ho
- Special Histological Type of Synchronous Primary Lung Cancer.....286~290  
Hui-Ju Ho, Wei-Heng Hung, Bing-Yen Wang

# Effect of N-acetylcysteine on Acid Aspiration Followed by Ventilator-Induced Acute Lung Injury in a Rat Model

Hung-Tze Tay\*, Khee-Siang Chan\*, Chin-Ming Chen\*,\*\*

**Introduction:** To examine the pharmacological effects of N-acetylcysteine (NAC) in a 2-hit rat model of acid aspiration-induced inflammation followed by ventilator-induced lung injury (VILI).

**Methods:** Rats received intra-tracheal instillation of hydrochloric acid as a first hit to induce systemic inflammation. For the second hit, they were randomized to receive mechanical ventilation (MV) using 1 of 2 strategies: a high tidal volume (TV) of 15 mL/kg and zero positive end-expiratory pressure (PEEP), or a protective strategy of a low TV of 6 mL/kg and a PEEP of 5 cm H<sub>2</sub>O. Rats in both groups were exposed to a fraction of inspired oxygen (FiO<sub>2</sub>) level of 40% during the 4-hour experimental period. Intravenous bolus of NAC (150 mg/kg) or placebo was administered 30 minutes before the different MV strategies. The following variables were measured: blood gases, lung mechanics (static compliance and respiratory elastance), lung edema, extended lung destruction (lung injury scores and lung histology), neutrophil recruitment in the lung and cytokine/chemokine production.

**Results:** Hemodynamics including blood pressure and heart rates did not differ between groups at baseline and during the study period. Compared to the placebo-treated rats, those administered NAC presented attenuated lung injury, as evidenced by improved oxygenation, preserved lung mechanics and diminished lung destruction and inflammation.

**Conclusion:** Using the 2-hit rat model, NAC administration was found to improve the physiologic and biologic profiles of rats in this experimental VILI model. (*Thorac Med* 2017; 32: 245-258)

Key words: acid aspiration, inflammation, N-acetylcysteine, ventilator-induced lung injury

## Introduction

Acid aspiration pneumonitis initiated by inhaling low pH gastric fluid may be complicated by subsequent bacterial pneumonia [1]. Gastric fluid aspiration frequently occurs in trauma pa-

tients or in critical patients with head trauma, or in those who were victims of alcohol-induced or cerebrovascular accidents, and is also a common complication of general anesthesia that occurs in 1/2,000-3,000 cases when anesthetics are used [2]. When it is followed by lung injury

---

\*Department of Intensive Care Medicine, Chi Mei Medical Center, Tainan, Taiwan; \*\*Department of Recreation and Health-Care Management, Chia Nan University of Pharmacy and Science, Tainan, Taiwan  
Address reprint requests to: Dr. Chin-Ming Chen, Department of Intensive Care Medicine, Chi Mei Medical Center, No. 901, Chung-Hwa Road, Yang-Kang District, Tainan City, 71073, Taiwan (R.O.C)

with a severity ranging from mild, subclinical pneumonitis to progressive respiratory failure, acid aspiration can be an independent risk factor for the development of acute respiratory distress syndrome (ARDS) [1]. ARDS is a leading cause of death among critically ill patients; it results in pulmonary inflammation that is characterized by neutrophil recruitment and injuries to the endothelium and epithelium, leading to an increase in the permeability of alveolar capillaries and hypoxemia. Mechanical ventilation (MV) is generally used as a life-saving treatment [3]. But the over-distension of lung units, the shearing forces that are generated during repetitive opening and closing of atelectatic lung units, and biotrauma caused by inadequate MV settings may lead to mechanical stress that can result in ventilator-induced lung injury (VILI). Acid aspiration models can make the lung more susceptible to VILI and cause pneumonia by sequential insults, or a “2-hit injury” [4-6]. The disruption of endothelial and epithelial cells, increased endothelial and epithelial permeability, neutrophil infiltration, enhanced production of inflammatory or anti-inflammatory cytokines/chemokines, including interleukin (IL)-1 $\beta$ , IL-6, IL-8 (the equivalent of animal chemokine ligand 1, CXCL1), IL-10, and tumor necrosis factor (TNF)- $\alpha$ , and subsequent highly permeable pulmonary edema and hyaline membranes, and decreased lung compliance and oxygenation are included in the spectrum of injuries [4-7].

Though the clinical outcomes of patients with ARDS have improved through the use of a low tidal volume (TV) when using MV, many conscious patients with ARDS may not be given a protective lung MV strategy during their ICU stay [8-10]. Therefore, it is necessary to search for another promising therapy be-

sides protective strategies to manage ARDS. N-acetylcysteine (NAC), a glutathione precursor (GSH), is a thiol compound with the sulfhydryl group and acts as an antioxidant drug and as a chemical reductant of oxidized thiols; it functions as a scavenger of reactive oxygen species (ROS) and a regulator of the redox reaction, which modulates the gene expression and inflammatory reaction in cells [11]. NAC can also decrease the number of apoptotic cells and the glutathione disulfide (GSSG)/GSH ratio, thus exhibiting its antioxidant characteristics [12]. The beneficial effects of NAC on lung injury have been reported in various experimental scenarios, including endotoxemia, sepsis, oleic acid-induced lung injury, hemorrhagic shock and VILI, and have yielded evidence of diminished lung edema and cytokines response, as well as preserved respiratory mechanics and oxygenation [13-18]. These studies have shown that NAC prevented pulmonary edema and acute kidney injury in rats with sepsis subjected to MV [14]. Moreover, NAC attenuated VILI through a strategy of high TV (15 ml/kg) in an isolated and perfused rat lung model [16], and prevented damage from acid-induced lung injury [18]. NAC could also attenuate the tissue oxidative stress level and lung injury in a 2-hit model of trauma [19]. Based on these findings, we sought to assess the potential benefits of NAC administration in a rat model of 2-hit injury with acid aspiration-primed lung inflammation followed by VILI.

## Methods

### *Rat Preparation*

Our experimental protocols were approved by the Institutional Animal Care and Use Committee of Chi-Mei Hospital (CMFHR10314,

date of approval: Jan 1, 2014). Intraperitoneal injection of urethane (2 mg/kg; Sigma, St. Louis, MO, USA) was used to anesthetize male Sprague-Dawley rats (350-400 g) while in the supine position. An intravenous cannula was inserted into and maintained in the tail vein to sustain the effect of anesthesia through continuous infusion of ketamine (15 mg/kg/h), xylazine (3 mg/kg/h), and pancuronium (0.35 mg/kg/h), and infusion of lactated Ringer's solution. The right carotid artery was cannulated (Angiocath IV Catheter; 24-gauge) to monitor mean arterial pressure (MAP) and to collect samples for blood gas analysis (Ciba-Corning Model 248 blood gas analyzer; Corning Medical, Medfield, MA). Rectal temperature was maintained at  $37 \pm 0.5^\circ\text{C}$  using a heating pad during the study period.

A tracheostomy was created using a 14-gauge cannula (Angiocath IV Catheter, 2.1 × 48 mm; Becton Dickinson Infusion Therapy Systems, Inc., Sandy, UT, USA) inserted into the trachea. The animals were ventilated with a Servo 300 ventilator (Siemens, Solna, Sweden) using a TV setting of 6 ml/kg, positive end-expiratory pressure (PEEP) of 5 cmH<sub>2</sub>O, and a respiratory rate of 50 breaths/min with a fraction of inspired oxygen (FiO<sub>2</sub>) of 40%.

### ***Acid instillation***

Hydrochloric acid (HCl, pH 2.0) (referred to as "acid") at 0.4 mL/kg was instilled intra-tracheally using an intra-tracheal aerosolizer (Penn Century, Inc., Philadelphia, PA, USA). A recruitment maneuver to prevent lung collapse was performed immediately after acid administration by increasing PEEP levels to 25 cmH<sub>2</sub>O for 5 breaths using a Servo 300 ventilator (Siemens, Solna, Sweden). After ventilation for 5 min to stabilize the rats using the same

ventilator settings as described above, an arterial blood gas sample was taken. A PaO<sub>2</sub> range of 100-150 mmHg was considered as a standard for a model of ARDS; animals with a PaO<sub>2</sub> out of this range were not included in the study.

### ***Experimental Protocol***

NAC (150 mg/kg, NAC group) in lactated Ringer's solution or lactated Ringer's solution alone (placebo group) was administered in a 0.5 mL intravenous bolus 30 min before the randomization of different MV strategies (soon after inducing acid aspiration). Rats were observed for 30 min for stabilization after cannulation, and were then randomized into 4 groups in a blinded fashion. Group HV: rats ventilated with high TV + placebo; Group HVN: rats ventilated with high TV + NAC; Group LV: rats ventilated with low TV + placebo; and Group LVN: rats ventilated with LV + NAC. The HV/HVN groups were ventilated with a TV of 15 mL/kg and zero PEEP at a respiratory rate of 16-18 breaths/min. The LV/LVN groups were ventilated with a TV of 6 mL/kg and PEEP of 5 cmH<sub>2</sub>O at a rate of 45-55 breaths/min. FiO<sub>2</sub> was kept at 40%. We maintained the ventilator period for 4 h after randomization.

Two other groups, a naive control and acid aspiration alone without ventilation group served as time-matched controls. Thus, there were 6 groups with 10 animals each, including naive control animals without acid aspiration or ventilator (Naive), acid aspiration-challenged animals receiving no MV (Control), and the HV, HVN, LV and LVN groups.

### ***Measurements***

Heart rates and pulse oximeter (SpO<sub>2</sub>) were measured using a veterinary pulse co-oximeter (Nonin 8600, Plymouth, MN) before acid instil-

lation and hourly after randomization. Airway pressures (plateau pressures) were recorded using a data acquisition system (National Instrument DAQCard 700, Austin, TX) at a sampling rate of 200 Hz (ICU Lab, KleisTEK Engineering, Bari, Italy). Lung elastance was calculated using the following formula: (Plateau Pressure-PEEP)/TV. Plateau pressure was measured hourly at the end of a 3 to 4 s end-inspiratory occlusion; PEEP was measured at the end of a 3 to 4 s end-expiratory occlusion. Blood gases were measured at the beginning of the randomization and hourly thereafter.

We sacrificed the rats using sodium pentobarbital overdosing. Their lungs were excised via a midline sternotomy and static pressure-volume curves were generated by manually injecting 0.5 to 1 cm<sup>3</sup> aliquots of air in a stepwise manner, starting at atmospheric pressure and continuing until an airway pressure of 30 cmH<sub>2</sub>O was achieved. The lungs subsequently were deflated, using a similar stepwise approach. Volumes were maintained for 6 s at each step of air inflation or deflation. The right upper lungs were used to measure wet-to-dry (W/D) lung weight ratios. The left lung was lavaged (bronchoalveolar lavage, BAL) for cell differentiation determinations. Cytokine/chemokine concentrations (IL-1 $\beta$ , IL-6, IL-10, CXCL1, and TNF- $\alpha$ ) in plasma and BAL fluid samples (n=10 in each group) were determined in a blinded fashion by technicians using Duo-Set ELISA Development kits (R&D Systems, Minneapolis, MN, USA).

### **Lung Histology**

The histology and lung injury assessments of the right lungs were evaluated by a pathologist who was blinded to the experimental groups, using the methods described previously.

These include neutrophil counts (A) in the alveoli and (B) interstitial spaces (score 0 if no neutrophils; score 1 if 1-5 neutrophils; score 2 if >5 neutrophils); (C) hyaline membranes (score 0 if none; score 1 if 1 membrane; score 2 if >1 membranes); (D) proteinaceous debris that filled airspaces (score 0 if none; score 1 if 1 debris; score 2 if >1 debris); and (E) alveolar septal thickening (score 0 if <2 times; score 1 if 2-4 times; score 2 if >4 times) [20]. For each lung histology slide, 5 regions were examined. The score was calculated as [(20×A) + (14×B) + (7×C) + (7×D) + (2×E)]/(number of fields×100). The resulting injury score was a value between 0 and 1.

### **Statistical Analysis**

Data are shown as means  $\pm$  standard errors. Groups were compared using 1-way analysis of variance (ANOVA). Post-hoc pairwise comparisons were performed using Bonferroni's multiple comparisons test. Statistical analysis was done using SPSS 13.0 software (SPSS Inc. Chicago, IL, USA). The significance level was set at  $\alpha=0.05$ .

## **Results**

### **Hemodynamic status**

The volumes of infused fluid were identical ( $\approx$ 2.5 mL of lactated Ringer's solution) for all rats during the MV period. Four hours after ventilator use, a similar hemodynamic status (MAP and heart rates) at baseline and during MV was observed in each group of rats (Table 1).

### **Blood Gas Analysis, Respiratory Mechanics, Lung Wet-to-Dry Ratios, Cell Counts in Bronchoalveolar Lavage Fluids, and Lung Injury**

Table 1. Hemodynamics and Blood Gas Analysis (n=10~15 per group)

	Baseline	60 min	120 min	180 min	240 min
<b>Heart rate (min<sup>-1</sup>)</b>					
HV	420.9 ± 8.1	418.9 ± 5.7	412.1 ± 5.5	414.4 ± 3.1	413.3 ± 4.5
HVN	421.4 ± 6.0	419.7 ± 4.5	419.2 ± 5.3	412.3 ± 3.0	415.5 ± 3.5
LV	420.0 ± 6.2	425.8 ± 7.0	413.2 ± 3.5	415.2 ± 7.3	414.5 ± 7.3
LVN	418.5 ± 7.3	416.6 ± 5.9	416.3 ± 4.2	415.4 ± 3.4	416.0 ± 3.4
<i>p</i> value	0.992	0.842	0.917	0.959	0.971
<b>MAP (mmHg)</b>					
HV	106.3 ± 1.3	102.8 ± 1.1	100.4 ± 1.3	101.1 ± 1.6	97.6 ± 1.4
HVN	107.4 ± 2.3	102.2 ± 1.6	101.3 ± 1.0	100.5 ± 1.4	97.4 ± 1.4
LV	105.9 ± 3.1	101.9 ± 2.0	104.7 ± 2.7	101.9 ± 3.0	95.9 ± 2.7
LVN	109.0 ± 3.5	102.4 ± 1.9	105.2 ± 1.3	99.8 ± 2.0	97.6 ± 2.3
<i>p</i> value	0.967	0.993	0.927	0.981	0.943
<b>pH</b>					
HV	7.36 ± 0.01	7.39 ± 0.01	7.37 ± 0.01	7.36 ± 0.01	7.37 ± 0.01
HVN	7.35 ± 0.01	7.37 ± 0.01	7.37 ± 0.01	7.39 ± 0.01	7.40 ± 0.01
LV	7.34 ± 0.01	7.39 ± 0.01	7.39 ± 0.01	7.40 ± 0.01	7.42 ± 0.01
LVN	7.35 ± 0.01	7.37 ± 0.01	7.39 ± 0.01	7.39 ± 0.01	7.40 ± 0.01
<i>p</i> value	0.947	0.885	0.897	0.448	0.881
<b>PaCO<sub>2</sub> (mmHg)</b>					
HV	41.3 ± 0.9	39.9 ± 0.8	41.8 ± 0.9	41.5 ± 0.7	39.5 ± 1.0
HVN	43.6 ± 0.7	41.1 ± 1.1	41.9 ± 0.7	40.4 ± 0.8	38.7 ± 0.9
LV	41.0 ± 1.2	42.1 ± 0.9	40.3 ± 0.9	39.5 ± 0.9	38.8 ± 0.9
LVN	42.2 ± 0.9	41.1 ± 0.8	40.8 ± 0.9	39.4 ± 0.9	38.8 ± 0.8
<i>p</i> value	0.261	0.361	0.440	0.259	0.917
<b>HCO<sub>3</sub><sup>-</sup> (meq/L)</b>					
HV	23.5 ± 0.6	23.6 ± 0.5	23.8 ± 0.5	23.5 ± 0.6	22.5 ± 0.4
HVN	24.3 ± 0.4	23.8 ± 0.6	24.3 ± 0.6	24.5 ± 0.5	23.2 ± 0.8
LV	24.0 ± 0.5	23.5 ± 0.6	22.9 ± 0.6	23.2 ± 0.7	23.1 ± 0.8
LVN	23.3 ± 0.4	23.5 ± 0.4	23.7 ± 0.3	22.9 ± 0.5	22.9 ± 0.5
<i>p</i> value	0.467	0.968	0.304	0.255	0.891

HV: acid aspiration + high Vt; HVN: acid aspiration + high Vt + N-acetylcysteine; LV: acid aspiration + low Vt; LVN: acid aspiration + low Vt + N-acetylcysteine

### Scores

At baseline and during randomization for the 2 MV strategies, each group of rats had similar arterial pH, PaCO<sub>2</sub>, and HCO<sub>3</sub><sup>-</sup> values (Table

1). The mean PaO<sub>2</sub> values at baseline were similar for all rats (around 150 mmHg). However, these values were significantly lower in the HV group after MV for 120 min than in the other

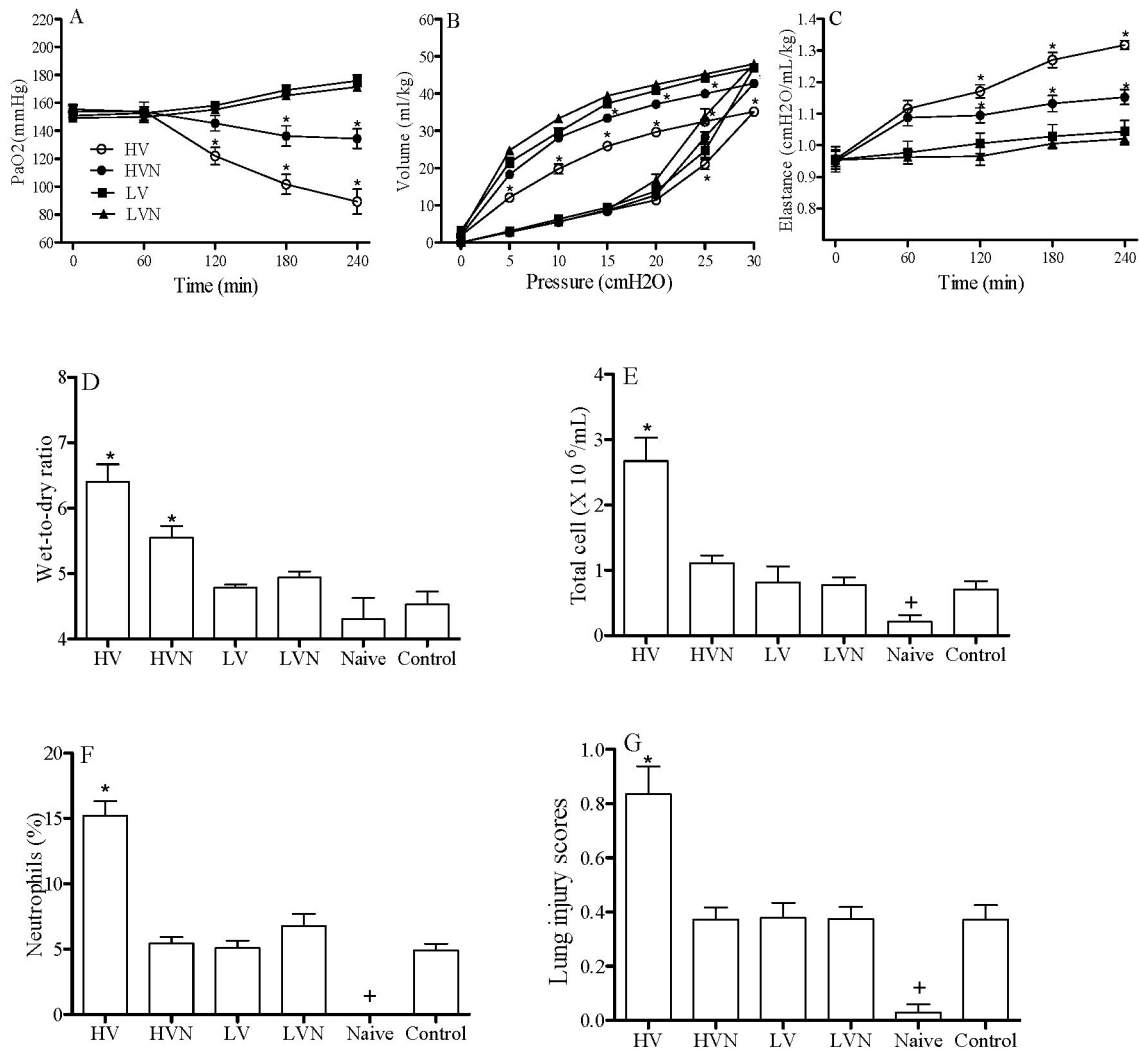


**Fig. 1.** Arterial blood gas (A) PaO<sub>2</sub> during 4 hours of MV after randomization. Static compliance curves (B) and lung elastance (C) at the end of the 4 hours of MV. The concave curves indicate inflation and the convex curves indicate deflation (B). Total cell counts (D) and neutrophil percentage (E) in bronchial lung lavage (BAL) fluids. (F) Lung wet-to-dry ratios. (G) Lung injury scores. \**p*<0.05 vs. other groups and †*p*<0.05 Naive vs. other group (*n*=10/group). Rat groups: HV: acid aspiration + high TV; HVN: acid aspiration + high TV + N-acetylcysteine; LV: acid aspiration + low TV; LVN: acid aspiration + low TV + N-acetylcysteine; Naive: naive control; Control: acid aspiration alone.

groups. The mean PaO<sub>2</sub> at 120 min was significantly lower in the HV group than in the HVN, LVN and LV groups (89.25 vs. 145.37, 155.15 and 158.07 mmHg, *p*<0.05) (Figure 1A). At the end of the study (240 min), the mean PaO<sub>2</sub> of the HV group was much lower than that of the HVN group (89.25 vs. 134.37 mmHg, *p*<0.05).

The HV and HVN groups both had significantly lower PaO<sub>2</sub> than the LVN and LV groups (89.25 and 134.37 vs. 171.46 and 175.80 mmHg, *p*<0.05) (Figure 1A). The HV group had the worst compliance of all the groups at the end of lung expansion with a pressure of 30 cmH<sub>2</sub>O, based on static pressure-volume curves (Fig-

ure 1B). Lung elastance values did not differ at baseline among all groups, but significantly increased in the HV group compared to the other groups after MV for 120 min. At 240 min of MV, the mean elastance was significantly higher in the HV than in the HVN group (1.31 vs. 1.15 cmH<sub>2</sub>O/mL/kg,  $p < 0.05$ ). The HV and HVN groups both had significantly higher mean elastance than the LVN and LV groups (1.31 and 1.15 vs. 1.02 and 1.04 cmH<sub>2</sub>O/mL/kg,  $p < 0.05$ ) (Figure 1C). These findings suggest that NAC administration improved oxygenation and compliance, and decreased elastance in rats treated with acid followed by high TV, but this was not the case in rats treated with acid followed by low TV.

The lung W/D ratios were significantly higher in the HV group than in the HVN group ( $6.40 \pm 0.27$  vs.  $5.54 \pm 0.18$ ,  $p < 0.05$ ). Both groups had significantly higher lung W/D ratios than the LV, LVN, Naïve and Control groups ( $4.78 \pm 0.05$ ,  $4.94 \pm 0.09$ ,  $4.30 \pm 0.32$  and  $4.52 \pm 0.21$ , respectively) (Figure 1D). Furthermore, BAL fluid total cell counts were significantly higher in the HV group ( $2.67 \pm 0.36 \times 10^6$ /mL) than in the other groups ( $1.11 \pm 0.12 \times 10^6$ /mL for HVN,  $0.81 \pm 0.26 \times 10^6$ /mL for LV,  $0.77 \pm 0.12 \times 10^6$ /mL for LVN,  $0.21 \pm 0.10 \times 10^6$ /mL for Naïve and  $0.71 \pm 0.12 \times 10^6$ /mL for Control) (Figure 1E). The HV group had a higher percentage of neutrophils in their BAL fluid (Figure 1F) and higher lung injury scores (Figure 1G) than the other groups. These findings indicate that NAC administration attenuated lung inflammation and injury in rats treated with acid followed by high TV, but not in rats treated with acid followed by low TV.

### **Cytokine/Chemokines Profiles**

The HV group had significantly higher

plasma levels of IL-1 $\beta$ , IL-6 and IL-10 than the HVN, LV, LVN, Naïve and Control groups (Figure 2). Moreover, levels of these cytokines were significantly higher in the LV group than in the LVN, Naïve and Control groups (Figure 2), and plasma levels of CXCL1 and TNF- $\alpha$  were higher in HV group than in the other groups (Figure 2). Levels of these cytokines/chemokines were also measured in BAL fluid. We found consistently that the HV group had significantly higher BAL levels of TNF- $\alpha$ , IL-6, IL-10 and CXCL1 than the other groups (Figure 3). However, there was no difference in IL-1 $\beta$  levels among the groups (Figure 3). In addition, BAL levels of these cytokines/chemokines did not differ between the LV and LVN groups (Figure 3). These findings indicate that NAC treatment reduced systemic inflammation in rats treated with acid followed by high and low TV, but reduced only lung inflammation in rats of the HV group.

### **Lung Histology**

As shown in Figure 4, the HV group had elevated neutrophil infiltration in the alveolar and interstitial spaces, increased hyaline membrane formation and proteinaceous debris accumulation within air spaces, and aggravated alveolar septal thickening, compared to the HVN group (Figure 4). However, the extent of lung injury did not appear to be different between the LV and LVN groups (Figure 4). These findings were consistent with the observations of W/D ratios, total cell counts and percentage of neutrophils in BAL fluid, lung injury scores, and lung elastance and static compliance.

### **Discussion**

Aspiration-induced lung injury is often un-

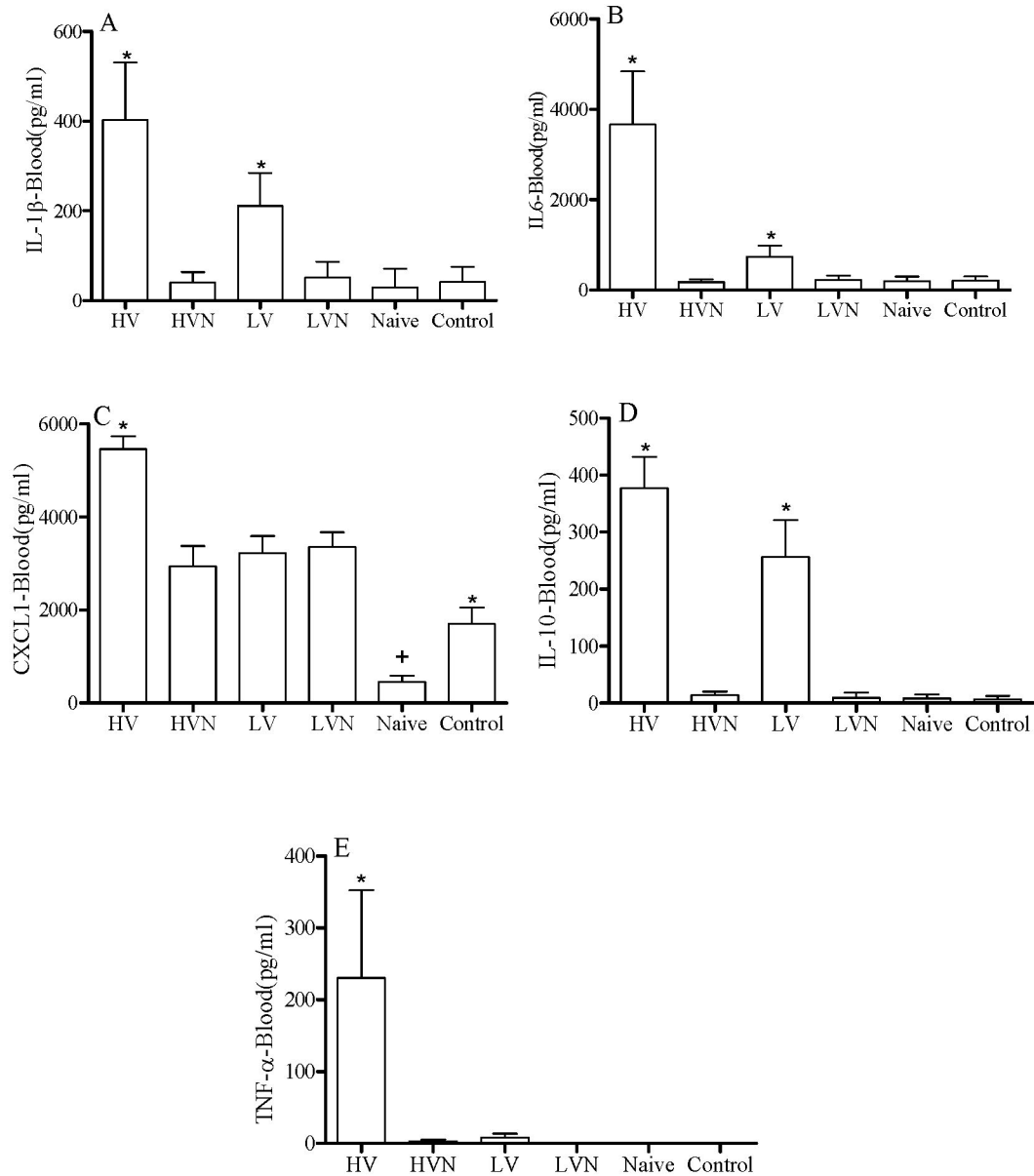


**Fig. 2.** Plasma cytokine/chemokines levels. \* $p < 0.05$  vs. other groups and  $^{\dagger} p < 0.05$  Naive vs. other groups ( $n = 10/\text{group}$ ). Rat groups: HV, acid aspiration + high TV; HVN, acid aspiration + high TV + N-acetylcysteine; LV, acid aspiration + low TV; LVN, acid aspiration + low TV + N-acetylcysteine; Naive, naive control; Control, acid aspiration alone.

derdiagnosed in the care of critically ill patients with altered consciousness, and may account for a significant proportion of acute pulmonary dysfunction and the subsequent development of pneumonia, lung injury or ARDS [1]. Inflammatory cellular responses such as neutrophils

recruitment, proinflammatory cytokines such as IL-1 $\beta$ , IL-6, and TNF- $\alpha$ , and chemokines such as IL-8 (the equivalent of animal CXCL1 in our study) are elevated following acid-induced lung injury [1,20-22]. MV is often necessary after acid aspiration, but it promotes lung injury, in-

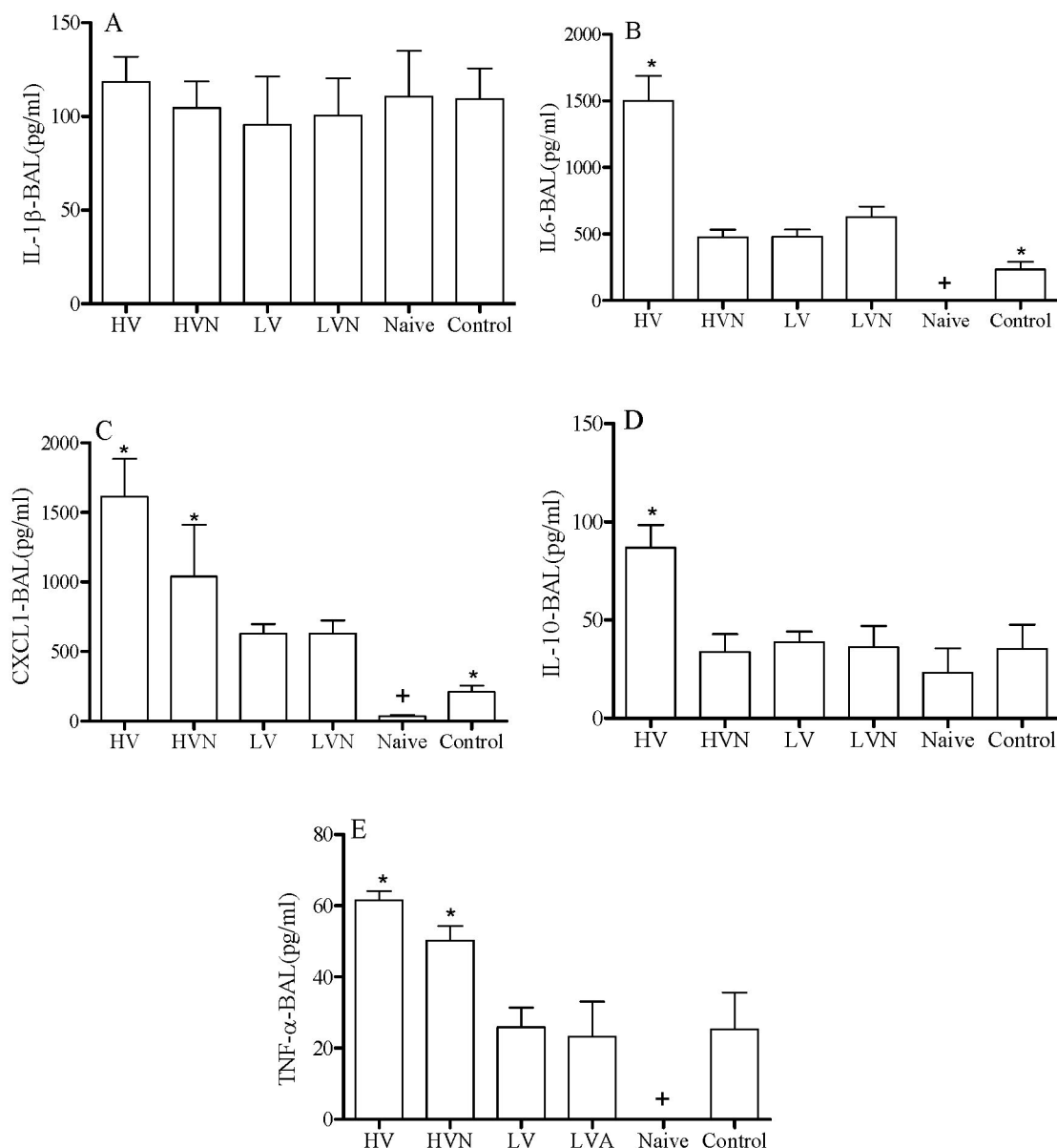


**Fig. 3.** Cytokine/chemokine levels in BAL. \* $p < 0.05$  vs. other groups and † $p < 0.05$  Naive vs. other groups ( $n = 10/\text{group}$ ). Rat groups: HV, acid aspiration+high TV; HVN, acid aspiration + high TV + N-acetylcysteine; LV, acid aspiration + low TV; LVN, acid aspiration + low TV + N-acetylcysteine; Naive, naive control; Control, acid aspiration alone.

cluding impaired oxygenation and lung compliance, with pronounced structural changes due to the excessive stretch applied to the aerated parenchyma [6,22-24]. In addition, IL-10 can be elevated during VILI [4]. IL-10 was originally described as a cytokine synthesis inhibitory

factor produced by Th2 cells that inhibits Th1 function. Many of the early studies on IL-10 focused on its ability to inhibit the production of IL-1 and TNF- $\alpha$  as anti-inflammatory cytokines. In fact, a major stimulus for the production of IL-10 is inflammation itself, because IL-1 and

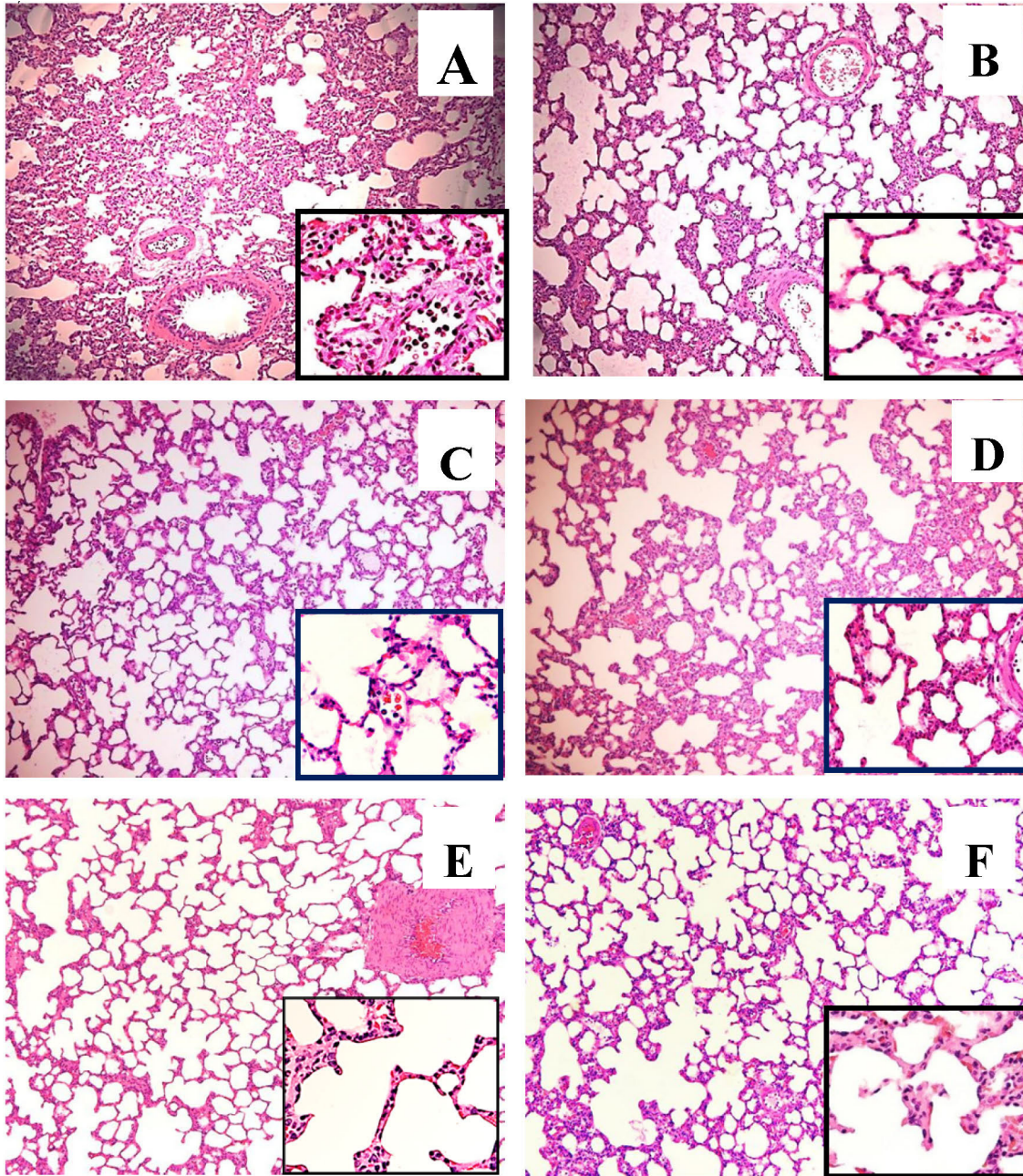


**Fig. 4.** Representative lung histology images (original magnification  $\times 100/400$ ). (A) HV, acid aspiration + high TV; (B) HVN, acid aspiration + high TV + N-acetylcysteine; (C) LV, acid aspiration + low TV; (D) LVN, acid aspiration + low TV + N-acetylcysteine. (E) Naive, naive control; and (F) Control, acid aspiration alone.

TNF- $\alpha$  can stimulate IL-10 production directly, suggesting the existence of a negative feedback loop whereby inflammatory processes are self-limited by the endogenous production of IL-

10 [25]. Taken together, these findings suggest that the magnitude of the endogenous IL-10 response correlates with both the severity of the inflammatory insult and the concentrations

of proinflammatory cytokines such as TNF- $\alpha$  [26]. Compared to the LV group and acid aspiration alone, the present study found that acid aspiration-primed lung inflammation followed by high TV significantly increased levels of cytokines/chemokines in the blood and BAL (IL-1 $\beta$ , IL-6, TNF- $\alpha$ , IL-10 and CXCL1), impaired lung mechanics, elevated the inflammatory cellular response and worsened oxygenation.

It has been noted that low TV reduces epithelial and endothelial injury in acid-injured rat lungs, and that the clinical outcome of patients with ARDS has been improved by the application of reduced TV [8,27]. Since the protective lung strategy is not implemented in all patients with ARDS, another rescue therapy such as NAC may be considered to attenuate possible lung injury [9-11]. We found no significant changes in mean arterial pressure, heart rate and blood gas analyses (except for improvement in oxygenation in VILI) after NAC treatment, suggesting that the use of NAC does not compromise hemodynamics and pulmonary function. Besides, NAC is one of the most widely investigated agents that serves as GSH and also acts as a direct scavenging agent. NAC can modulate gene expression, decrease cytokine production and apoptosis, down-regulate the expression of adhesion molecules, restore nitric oxide production, restore the antioxidant potential of cells, decrease bacterial translocation, and reduce ROS production, thus improving survival [12,14,16,28-30]. It was also noted in previous studies that NAC can improve alveolar edema via sodium transport from alveolar epithelial clearance [29-31]. Campos *et al.* also reported that in a rat model of sepsis submitted to MV with low TV, NAC prevented pulmonary edema and kidney injury, decreased oxidative stress and the edema index and improved the survival

rate [14]. The above findings were consistent with our data of an improvement in lung edema through decreased W/D ratios. In addition, in the VILI model of isolated and perfused rat lung, Chiang *et al.* found that NAC can increase GSH, and attenuate ROS (an important role in the pathogenesis of VILI), cytokines response (IL-1 $\beta$  and TNF- $\alpha$ ) and lung permeability [16]. NAC was also proved to attenuate lung injury in a 1-hit model of endotoxemia, hemorrhagic shock, sepsis, acid-induced lung injury, VILI or meconium aspiration [13-18]. In the present study, we found that the administration of NAC attenuated lung injury and systemic inflammation in a 2-hit rat model of acid aspiration followed by VILI. However, the therapeutic benefits could not be observed in rats treated with acid followed by a low TV. This reflects the protective role of a low TV in VILI, leading to decreased lung edema, neutrophil accumulation, and lung injury and inflammation.

The production of cytokines and chemokines, oxidative bursts, and the release of proteolytic enzymes by neutrophil activation is largely responsible for lung injury [8]. An infiltration of PMNs in lung tissues and subsequent lipid peroxidation increased the production of TNF- $\alpha$  and IL-1 $\beta$ , and all parameters of inflammation were attenuated by NAC treatment due to inhibition of neutrophil sequestration in the lungs [32]. In the model of oleic acid-induced lung injury, NAC treatment was also related to preservation of lung architecture and decreased neutrophil accumulation as reduced myeloperoxidase activity in lung tissue [18]. Our result revealed that NAC administration significantly suppressed neutrophil infiltration and activity.

The study has several limitations. First, we did not measure the concentration of NAC, GSSH/GSH and antioxidants in the lung or

blood. This data would provide a reliable measure of the antioxidant profile, and can be done in future studies. Second, the sample and body size were small, so the conclusions must be taken cautiously, and extrapolating these results to clinical situations would be difficult. Third, we administered NAC before the onset of MV to maximize the protective effect; therefore, the use of late treatment with NAC is warranted for future studies. Fourth, we used a single NAC dosage of 150 mg/kg and an experimental 4-hour MV protocol; therefore, further studies should consider using other NAC dosages, such as 600 or 1,200 mg, and longer experimental protocols to determine the best therapeutic window of NAC.

## Conclusion

In conclusion, the results of this study suggest that NAC treatment had a promising role as an adjunctive modality in a clinical 2-hit model of acid aspiration followed by VILI, as evidenced by the improved physiologic and biologic profiles. Further advanced experimental and clinical studies on this subject are necessary.

## References

1. Raghavendran K, Nemzek J, Napolitano LM, *et al.* Aspiration-induced lung injury. *Crit Care Med* 2011; 39: 818-26.
2. Marik PE. Aspiration pneumonitis and aspiration pneumonia. *N Engl J Med* 2001; 344: 665-71.
3. Rubenfeld GD, Caldwell E, Peabody E, *et al.* Incidence and outcomes of acute lung injury. *N Engl J Med* 2005; 353: 1685-93.
4. Chen CM, Penuelas O, Quinn K, *et al.* Protective effects of adenosine A2A receptor agonist in ventilator-induced lung injury in rats. *Crit Care Med* 2009; 37: 2235-41.
5. Chen CM, Cheng KC, Li CF, *et al.* The protective effects of glutamine in a rat model of ventilator-induced lung injury. *J Thorac Dis* 2014; 6: 1704-13.
6. Lai CC, Liu WL, Chen CM. Glutamine attenuates acute lung injury caused by acid aspiration. *Nutrients* 2014; 6: 3101-16.
7. Slutsky AS, Ranieri VM. Ventilator-induced lung injury. *N Engl J Med* 2013; 369: 2126-36.
8. Ventilation with lower tidal volumes as compared with traditional tidal volumes for acute lung injury and the acute respiratory distress syndrome. The Acute Respiratory Distress Syndrome Network. *N Engl J Med* 2000; 342: 1301-8.
9. Gajic O, Dara SI, Mendez JL, *et al.* Ventilator-associated lung injury in patients without acute lung injury at the onset of mechanical ventilation. *Crit Care Med* 2004; 32: 1817-24.
10. Ferguson ND. Low tidal volumes for all? *JAMA* 2012; 308: 1689-90.
11. Atkinson MC. The use of N-acetylcysteine in intensive care. *Crit Care Resusc* 2002; 4: 21-7.
12. Grosicka-Maciag E, Kurpios-Piec D, Szumilo M, *et al.* Protective effect of N-acetyl-L-cysteine against maneb-induced oxidative and apoptotic injury in Chinese hamster V79 cells. *Food Chem Toxicol* 2011; 49: 1020-5.
13. Choi JS, Lee HS, Seo KH, *et al.* The effect of post-treatment N-acetylcysteine in LPS-induced acute lung injury of rats. *Tuberc Respir Dis (Seoul)* 2012; 73: 22-31.
14. Campos R, Shimizu MH, Volpini RA, *et al.* N-acetylcysteine prevents pulmonary edema and acute kidney injury in rats with sepsis submitted to mechanical ventilation. *Am J Physiol Lung Cell Mol Physiol* 2012; 302: L640-50.
15. Forgiarini LF, Forgiarini LA, Jr., *et al.* N-acetylcysteine administration confers lung protection in different phases of lung ischaemia-reperfusion injury. *Interact Cardiovasc Thorac Surg* 2014; 19: 894-9.
16. Chiang CH, Chuang CH, Liu SL, *et al.* N-acetylcysteine attenuates ventilator-induced lung injury in an isolated and perfused rat lung model. *Injury* 2012; 43: 1257-63.
17. Mokra D, Drgova A, Petras M, *et al.* N-acetylcysteine alleviates the meconium-induced acute lung injury. *Adv Exp Med Biol* 2015; 832: 59-67.
18. Koksel O, Cinel I, Tamer L, *et al.* N-acetylcysteine inhibits peroxynitrite-mediated damage in oleic acid-

- induced lung injury. *Pulm Pharmacol Ther* 2004; 17: 263-70.
19. Gurer A, Ozdogan M, Gokakin AK, *et al.* Tissue oxidative stress level and remote organ injury in two-hit trauma model of sequential burn injury and peritoneal sepsis are attenuated with N-acetylcysteine treatment in rats. *Ulus Travma Acil Cerrahi Derg* 2009; 15: 1-6.
  20. Matute-Bello G, Downey G, Moore BB, *et al.* Acute Lung Injury in Animals Study G: An official American Thoracic Society workshop report: features and measurements of experimental acute lung injury in animals. *Am J Respir Cell Mol Biol* 2011; 44: 725-38.
  21. Pawlik MT, Schubert T, Hopf S, *et al.* The effects of fenoterol inhalation after acid aspiration-induced lung injury. *Anesth Analg* 2009; 109: 143-50.
  22. Khalife-Hocquemiller T, Sage E, Dorfmuller P, *et al.* Exogenous surfactant attenuates lung injury from gastric acid aspiration during ex vivo reconditioning in pigs. *Transplantation* 2014; 97: 413-8.
  23. Amigoni M, Bellani G, Zambelli V, *et al.* Unilateral acid aspiration augments the effects of ventilator lung injury in the contralateral lung. *Anesthesiology* 2013; 119: 642-51.
  24. Kuiper JW, Plotz FB, Groeneveld AJ, *et al.* High tidal volume mechanical ventilation-induced lung injury in rats is greater after acid instillation than after sepsis-induced acute lung injury, but does not increase systemic inflammation: an experimental study. *BMC Anesthesiol* 2011; 11: 26.
  25. van der Poll T, Jansen J, Levi M, *et al.* Regulation of interleukin 10 release by tumor necrosis factor in humans and chimpanzees. *J Exp Med* 1994; 180: 1985-8.
  26. Scumpia PO, Moldawer LL. Biology of interleukin-10 and its regulatory roles in sepsis syndromes. *Crit Care Med* 2005; 33: S468-71.
  27. Frank JA, Gutierrez JA, Jones KD, *et al.* Low tidal volume reduces epithelial and endothelial injury in acid-injured rat lungs. *Am J Respir Crit Care Med* 2002; 165: 242-9.
  28. Ritter C, Andrades ME, Reinke A, *et al.* Treatment with N-acetylcysteine plus deferoxamine protects rats against oxidative stress and improves survival in sepsis. *Crit Care Med* 2004; 32: 342-9.
  29. Zafarullah M, Li WQ, Sylvester J, *et al.* Molecular mechanisms of N-acetylcysteine actions. *Cell Mol Life Sci* 2003; 60: 6-20.
  30. Dickie AJ, Rafii B, Piovesan J, *et al.* Preventing endotoxin-stimulated alveolar macrophages from decreasing epithelium Na<sup>+</sup> channel (ENaC) mRNA levels and activity. *Pediatr Res* 2000; 48: 304-10.
  31. Modelska K, Matthay MA, Brown LA, *et al.* Inhibition of beta-adrenergic-dependent alveolar epithelial clearance by oxidant mechanisms after hemorrhagic shock. *Am J Physiol* 1999; 276: L844-57.
  32. Cuzzocrea S, Mazzon E, Dugo L, *et al.* Protective effects of n-acetylcysteine on lung injury and red blood cell modification induced by carrageenan in the rat. *FASEB J* 2001; 15: 1187-200.

## 乙醯半胱胺酸在大白鼠模式下對酸吸入後伴隨呼吸器引發之急性肺損傷的作用

鄭鴻志\* 陳奇祥\* 陳欽明\*,\*\*

**前言：**檢視乙醯半胱胺酸在酸吸入造成之肺發炎後伴隨呼吸器引發之肺損傷的動物模式下之藥理作用。

**方法：**大白鼠先接受氣管內注射鹽酸造成全身性發炎的一度傷害，之後再隨機接受兩種不同的呼吸器模式以造成二度傷害，包括 15 毫升/公斤之高潮氣容積合併零吐氣末正壓造成呼吸器引發肺損傷，或是 6 毫升/公斤之低潮氣容積合併 5 公分水柱吐氣末正壓之保護性呼吸器模式。實驗期間皆供應 40% 氧氣濃度及 4 個小時呼吸器使用。在實驗開始前 30 分鐘，先從靜脈投予乙醯半胱胺酸（150 毫克/公斤）或是林格式液（對照組）。過程中監測以下參數：動脈血、肺靜態順應性、呼吸系統彈性、肺水腫、瀰漫性肺傷害嚴重度（肺傷害分數及肺組織病變）、肺泡內嗜中性白血球數及細胞激素/化學激素濃度。

**結果：**實驗開始及過程中各組老鼠之血壓及心跳無顯著差異。跟對照組相比，注射乙醯半胱胺酸能夠減輕大白鼠之肺損傷，包括改善氧合、改善肺靜態順應性及呼吸系統彈性、減輕肺破壞、以及減少全身性發炎。

**結論：**根據本實驗，乙醯半胱胺酸注射可以改善大白鼠肺損傷模式下之生理及生物參數。（*胸腔醫學* 2017; 32: 245-258）

**關鍵詞：**胃酸吸入，發炎，乙醯半胱胺酸，呼吸器引發肺損傷

---

\* 財團法人奇美醫學中心 加護醫學部，\*\* 嘉南藥理科技大學 休閒管理系

索取抽印本請聯絡：陳欽明醫師，奇美醫學中心 加護醫學部，71073 台南市永康區中華路 901 號

# Pulmonary Benign Metastasizing Leiomyoma: A Case Presentation and Review of the Literature

You-Cheng Jiang\*, Min-Hsi Lin\*, Ruay-Sheng Lai\*\*,\*\*

Uterine leiomyoma is a common benign tumor in women of reproductive age. In rare cases, distant metastasis can develop months to years after gynecological procedures. Metastasis to the lung, or pulmonary benign metastasizing leiomyoma (PBML), is the most common type. Patients are usually asymptomatic and the tumor is found incidentally on routine chest x-ray. The typical radiological presentation is multiple pulmonary nodules. Management includes observation, surgery, or hormonal manipulation. There is increasing evidence of partial regression of PBML with the use of hormone therapy. We report the case of a 46-year-old woman who presented with diffuse lung cysts complicated by pneumothorax. In this case, a decreasing cyst size and number were observed after only 3 months of hormone therapy. (*Thorac Med* 2017; 32: 259-265)

Key words: pulmonary benign metastasizing leiomyoma, pneumothorax, hormone therapy

## Introduction

Pulmonary benign metastasizing leiomyoma (PBML) is a rare condition in which a benign uterine fibroid metastasizes to the lung. Pulmonary metastasis usually develops months to years after total hysterectomy or myomectomy. The median age at diagnosis is 46.5 years. Bilateral pulmonary nodules are the typical radiographic findings. Only 3 published case reports have described cystic lung disease associated with this condition [1,9,13]. Management has not been standardized, and may involve observation, surgery, or hormonal manipulation.

Herein, we report a patient with PBML presenting with multiple lung cysts complicated by pneumothorax. The patient showed a partial response to hormone therapy, even with extensive lung parenchymal destruction.

## Case Report

A 46-year-old woman presented with a sudden onset of breathlessness for 1 day. She had undergone hysterectomy approximately 4 years earlier, and a chronic cough developed 1 year later. At that time, she visited a chest clinic, where chest radiograph revealed bilateral lung

---

\*Division of Chest Medicine, Department of Internal Medicine, Kaohsiung Veterans General Hospital, Kaohsiung, Taiwan; \*\*National Yang-Ming University School of Medicine, Taipei, Taiwan

Address reprint requests to: Dr. Min-Hsi Lin, Division of Chest Medicine, Department of Internal Medicine, Kaohsiung Veterans General Hospital, No. 386, Dazhong 1st Rd., Zuoying Dist., Kaohsiung City, 81362, Taiwan, R.O.C.

nodules (Figure 1A). Chest computed tomography (CT) showed bilateral multiple polygonal cysts and well-defined low-density nodules (Figure 1B). She refused lung biopsy and chose a wait-and-see strategy with a presumptive diagnosis of PBML. She had irregular follow-up after that without chest radiography.

The patient had been in her usual state of health until 1 day prior to the current admission, when she experienced an abrupt onset of chest pain associated with shortness of breath and the development of a cold sweat. The chest pain was sharp and localized without radiation to the shoulder. She denied any fever, audible wheeze, orthopnea, or prolonged immobilization. The patient then visited the emergency department because of persistent breathlessness.

At presentation, the patient appeared acutely ill. Her blood pressure was 151/92 mmHg, pulse 95 beats per minute, respiration rate 19 breaths per minute, and oxygen saturation by pulse oximetry 94% with an oxygen flow rate of 3 L/min by nasal cannula. Auscultation revealed diminished left breathing sounds. Laboratory tests were unremarkable. Chest radiograph showed left pneumothorax (Figure 2) and an increased size and number of multiple bilateral pulmonary nodules. The cysts were also significantly enlarged on chest CT. A pigtail catheter was placed, but the air-leak persisted. The patient underwent video-assisted thoracoscopic surgery (VATS) for wedge resection of the left bullae, followed by chest tube placement. Microscopy revealed cystic tissue and nodules of bland spindle cells, which were positive for smooth muscle actin (SMA), estrogen receptor (ER), progesterone receptor (PR), h-caldesmon and B-cell lymphoma 2 (BCL2), and negative for homatropine methylbromide 45 (HMB-45). PBML was pathologically confirmed. Hormone



**Fig. 1A.** Chest radiograph showing multiple nodules in both lungs 3 years before this presentation.



**Fig. 1B.** Chest CT showing multiple irregular polygonal-shaped cysts and well-defined nodules. Neither reticular opacity nor honeycomb was found.

therapy with a gonadotropin-releasing hormone analogue (leuprorelin) was then administered. Full expansion of the left lung and partial regression of the cysts and nodules were observed on the follow-up chest x-ray 3 months later (Figure 3).



**Fig. 2.** Chest radiography showing pneumothorax of the left lung. Increased reticulonodular pattern and cyst formation were also noticed in the right lung.



**Fig. 3.** Follow-up chest x-ray revealed partially regressed cysts and nodules after 3 months of hormone therapy.

## Discussion

Uterine fibroids are the most common benign pelvic tumor in reproductive-aged women. Nevertheless, fewer than 150 cases of PBML from fibroids have been reported in the literature. Since the introduction of the diagnosis by Steiner in 1939, most reports have been small case series [2], and the exact incidence remains unknown. The median age at diagnosis is 46.5 years [3-4]. A majority of patients underwent hysterectomy or myomectomy for uterine leiomyoma prior to the development of PBML. The interval between operation and diagnosis ranged from 1 month to 36 years [4-5]. One proposed pathogenesis is the hematogenous spread of leiomyoma cells from the uterus during gynecological surgery, with subsequent colonization in pulmonary tissue. The lung is the most common

site of metastasis, but metastases to the lymph nodes, mediastinum, heart, abdomen, soft tissue, and bone have also been reported [7,11].

PBML is usually an incidental radiographic finding in asymptomatic patients, although cough, hemoptysis, chest pain, or dyspnea may occur. The most common radiographic pattern is multiple bilateral well-circumscribed solid nodules, which is observed in approximately 90% of cases [4]. The mean nodule size is 1.8 cm and the mean number of nodules is 6 [6]. PBML can also present as fluid-containing cysts mimicking hydatid cysts [8], cystic lung disease mimicking lymphangiomyomatosis [9], diffuse miliary nodules [10], cavitory nodules, or pleural involvement with effusion, although these are rare occurrences. Since there are no pathognomonic imaging signs, tissue biopsy diagnosis is required. The success rate of CT-

guided lung biopsy is only 66%, and a hospital review found that most patients underwent VATS [4]. A combination of clinical history and pathological reports is essential to the diagnosis.

PBML is composed of monomorphic well-differentiated spindle cells forming intersecting fascicles. Indicators of benign lesions are low mitotic activity (<5 mitoses per 10 high-power fields), low Ki-67 index, and a lack of nuclear atypia; in contrast, leiomyosarcoma has high mitotic activity. Immunohistochemical staining is positive for actin, desmin, and caldesmon. Estrogen and progesterone receptors are also expressed in the majority of cases [11], while leiomyosarcoma is negative for both. More important, HMB-45 has been found to be negative in all cases, thus distinguishing PBML from leiomyomatous hamartoma, perivascular epithelioid cell tumor, and lymphangioliomyomatosis [3].

Management of benign indolent disease is not standardized. Treatment modalities include a wait-and-see strategy, surgical resection of pulmonary nodules, oophorectomy with or without total abdominal hysterectomy, and hormonal manipulation. These options can be used alone or in combination, and sequentially or concurrently. No single approach is definitely effective and fits all cases. Appropriate management should take into consideration the radiographic presentation, speed of progression during follow-up, the patient's willingness to undergo surgery, and the response to initial treatment.

Surgery for resectable pulmonary nodules is curative. However, >90% of cases present as bilateral multiple nodules. The surgical removal of 87 nodules was reported in 1 case [12]; however, even the use of parenchyma-

sparing surgery to remove multiple nodules might cause concern. In the largest published review, comprising 57 PBML cases, only 20% of patients were able to undergo surgery with curative intent. In addition, approximately 80% of treatment-naïve patients showed stable disease within 2 years, and 72% of patients had unchanged disease for >2 years [4]. The nodules might spontaneously regress at menopause and after pregnancy [4]; hence, a wait-and-see strategy appears to be reasonable in cases of asymptomatic patients with a nodular presentation. However, cyst formation at diagnosis is a progressive process, resulting in extensive parenchymal destruction and pneumothorax, as in our case and in other case reports [1,9,13]. More aggressive treatment, either oophorectomy or hormone therapy, is required to preserve lung function and prevent life-threatening complications.

Hormonal manipulation has been advocated for several decades in patients who refused surgery or who had unresectable lesions [14]. Estrogen is a tumor promoter in uterine leiomyomas, and is responsible for fibroid growth during pregnancy. Estrogen and progesterone receptors are also expressed in approximately 90% of metastasizing leiomyomas [15]. Thus, attempts can be made to utilize estrogen receptor antagonists or to decrease estrogen production.

Tamoxifen and raloxifene are the currently available selective estrogen receptor modulators; these compounds have different effects on estrogen activity in different tissues. Tamoxifen shows no anti-tumor response because of its estrogen agonist effect on the myometrium. Raloxifene reduces tumor size in postmenopausal women; however, the effect is not consistent in premenopausal women [15].

An alternative approach is the reduction of estrogen, either through downstream ovary secretion or inhibition of *in situ* tumor production. Gonadotropin-releasing hormone (GnRH) agonists desensitize pituitary GnRH receptors by interrupting pulsatile stimulation. Downregulated follicle-stimulating hormone and luteinizing hormone decrease endogenous estrogen. Another approach is to inhibit the activity of aromatase, which converts androgen to estrogen and is overexpressed in some leiomyomas [16]. GnRH agonists or aromatase inhibitors decrease nodule size or prevent progression in 90% of cases [11]. Tumor size can decrease rapidly after 3 months of therapy. While some patients receive hormones for >1 year, the appropriate time to discontinue therapy has not yet been determined. Hormonal manipulation is gradually replacing oophorectomy as an effective treatment that does not sacrifice fertility. Oophorectomy should be reserved for tumors refractory to hormone therapy. However, only 1/3 of patients in a case series and review received hormone therapy [4].

PBML presenting as cystic lung disease is extremely rare. Our case demonstrates that lung cysts are progressive and require prompt intervention. Unlike in typical cases with a nodular presentation, a wait-and-see strategy might result in lung parenchymal destruction and pneumothorax. Hormone therapy is effective and can lead to reversal of pre-existing extensive cysts.

## References

1. Clément-Duchêne C, Vignaudb JM, Régent D, *et al.* Benign metastasizing leiomyoma with lung cystic lesions and pneumothoraces: A case report. *Respir Med CME* 2010; 3: 183-5.
2. Steiner PE. Metastasizing fibroleiomyoma of the uterus: Report of a case and review of literature. *Am J Pathol* 1939; 15: 89-110.
3. Patton KT, Cheng L, Papavero V, *et al.* Benign metastasizing leiomyoma: clonality, telomere length and clinicopathologic analysis. *Mod Pathol* 2006; 19: 130-40.
4. Miller J, Shoni M, Siegert C, *et al.* Benign metastasizing leiomyomas to the lungs: an institutional case series and a review of the recent literature. *Ann Thorac Surg* 2016; 101: 253-8.
5. Chen S, Lui RM, Li T. Pulmonary benign metastasizing leiomyoma: a case report and literature review. *J Thorac Dis* 2014; 6: E92-8.
6. Ağačkiran Y, Findik G, Ustün LN, *et al.* Pulmonary benign metastasizing leiomyoma: an extremely rare case. *Turk Patoloji Derg* 2016; 32: 193-5.
7. Awonuga AO, Shavell VI, Imudia AN, *et al.* Pathogenesis of benign metastasizing leiomyoma. *Obstet Gynecol Surv* 2010; 65: 189-95.
8. Alimi F, El Hadj Sidi C, Ghannouchi C. Cystic benign metastasizing leiomyoma of the lung mimicking hydatid cyst. *Lung* 2016; 194: 1029.
9. Matsumoto K, Yamamoto T, Hisayoshi T, *et al.* Intravenous leiomyomatosis of the uterus with multiple pulmonary metastases associated with large bullae-like cyst formation. *Pathol Int* 2001; 51: 396-401.
10. Orejola WC, Vaidya AP, Elmann EM. Benign metastasizing leiomyomatosis of the lungs presenting a miliary pattern. *Ann Thorac Surg* 2014; 98: e113-4.
11. Lewis EI, Chason RJ, DeCherney AH, *et al.* Novel hormonal therapy for the treatment of benign metastasizing leiomyoma: an analysis of 5 cases and literature review. *Fertil Steril* 2013; 99: 2017-24.
12. Otlakan A, Borda B, Lazar G, *et al.* Treatment decision based on the biological behavior of pulmonary benign metastasizing leiomyoma. *J Thorac Dis* 2016; 8: E672-6.
13. Hoetzenecker CK, Ankersmit HJ, Aigner C, *et al.* Consequences of a wait-and-see strategy for benign metastasizing leiomyomatosis of the lung. *Ann Thorac Surg* 2009; 87: 613-4.
14. Evans AJ, Wiltshaw E, Kochanowski SJ, *et al.* Metastasizing leiomyoma of the uterus and hormonal manipulations. Case report. *Br J Obstet Gynecol* 1986; 93: 646-8.
15. Palomba S, Orio F, Russo T, *et al.* Antiproliferative and

proapoptotic effects of raloxifene on uterine leiomyomas in postmenopausal women. *Fertil Steril* 2005; 84: 154-61.

16. Sumitani H, Shozu M, Segawa T, *et al.* In situ estrogen

synthesized by aromatase P450 in uterine leiomyoma cells promotes cell growth probably via an autocrine/intracrine mechanism. *Endocrinology* 2000; 141: 3852-61.

## 肺部良性轉移性平滑肌瘤－病例報告與文獻回顧

姜佑承\* 林旻希\* 賴瑞生\*,\*\*

子宮肌瘤是生育年齡女性最常見的良性腫瘤，然而接受子宮肌瘤切除手術的病患在數月或數年後卻可能罕見地出現遠端轉移；轉移至肺部最常見，此時稱為肺部良性轉移性平滑肌瘤。大部分病患都無症狀，直到意外在影像上發現肺結節才被診斷。治療的選項有追蹤、手術切除、以及荷爾蒙治療，荷爾蒙治療有越來越多成功的案例。我們報告一位46歲的女性病人，罕見的以肺囊腫併發氣胸來表現。本病患接受3個月荷爾蒙治療後，肺囊腫隨即變小與數量變少。( *胸腔醫學* 2017; 32: 259-265)

關鍵詞：肺部良性轉移性平滑肌瘤，氣胸，荷爾蒙治療

---

\* 高雄榮民總醫院 內科部 胸腔內科，\*\* 國立陽明大學

索取抽印本請聯絡：林旻希醫師，高雄榮民總醫院 內科部 胸腔內科，81362 高雄市左營區大中一路386號

# ***Candida* Pneumonia Diagnosed by Bronchoalveolar Lavage: A Case Report**

Wei-Hsin Hung, Kuang-Yao Yang\*,\*\*

Fungal pneumonia is difficult to diagnose in immunocompetent patients. Here, we report a case involving a male patient with no immunocompromised risk factors except old age, who was diagnosed with *Candida* pneumonia by bronchoalveolar lavage (BAL). Cytological examination of the BAL fluid showed that more than 2% of the recovered cells contained polymorphonuclear neutrophils and intracellular organisms. The final culture of the BAL fluid yielded *Candida albicans* without any bacterial growth. Fluconazole was then prescribed, but the patient suffered from acute respiratory distress syndrome and septic shock. The patient ultimately died, in spite of being in intensive care with mechanical ventilator support. (*Thorac Med* 2017; 32: 266-271)

Key words: *Candida* pneumonia, fungal pneumonia, bronchoalveolar lavage, leukocyte phagocytosis, intracellular microorganisms

## **Introduction**

Fungal pneumonia is extremely rare in immunocompetent patients, and the diagnosis is often difficult to reach. A biopsy followed by a histological examination is the most reliable method to diagnose fungal pneumonia. However, a sample is not always available for biopsy. Cytological evaluation of bronchoalveolar lavage (BAL) is an effective and quick method to diagnose fungal pneumonia. A cut-off value of 2% for intracellular organisms (ICO) in BAL fluid is typically considered proof of bacterial

pneumonia. However, specific cut-off values for fungi in BAL fluid are lacking [1]. In cases of lobar pneumonia that respond poorly to broad-spectrum antibiotics, clinicians should consider the possibility of fungal pneumonia.

## **Case Report**

An 88-year-old man presented to the emergency department with general weakness, poor appetite, and a productive cough with purulent sputum that had lasted for 1 week. The patient had hypertension and chronic eczema. Daily

---

Department of Chest Medicine, Taipei Veterans General Hospital, Taipei, Taiwan; \*Division of Respiratory Therapy, Department of Chest Medicine, Taipei Veterans General Hospital, Taipei, Taiwan; \*\*Institute of Emergency and Critical Care Medicine, School of Medicine, National Yang-Ming University, Taipei, Taiwan

Address reprint requests to: Dr. Kuang-Yao Yang, Division of Respiratory Therapy, Department of Chest Medicine, Taipei Veterans General Hospital, Taipei, Taiwan, No. 201, Sec. 2, Shih-Pai Rd., Beitou District, Taipei 11217, Taiwan, ROC



**Fig. 1.** Chest CXR showing a huge, thick-walled RUL cavitary lesion.

medications included felodipine and hydroxyzine. He was a non-smoker with no history of respiratory diseases such as asthma, bronchiectasis, or pulmonary tuberculosis. He had not recently traveled or been exposed to people with infectious diseases. There was no evident history of consumption of alcohol, illicit drugs, herbs, glucocorticoids, or immunosuppressants. Chest roentgenography (CXR) revealed fibrous changes with calcified nodules at the upper lung fields on both sides and a cavitary lesion at the right upper lobe (RUL) surrounded by focal consolidation (Figure 1). A RUL lung abscess was suspected initially. However, laboratory testing revealed leukocytosis with a white blood cell count of up to 28,000/cumm with a left shift and an elevated C-reactive protein level. Piperacillin/tazobactam were prescribed to treat the lung abscess, but progressive right upper and lower lobe consolidation was observed. The sputum culture yielded only yeast without

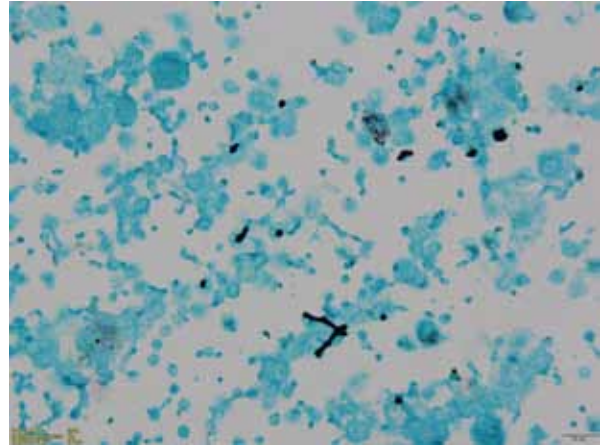


**Fig. 2.** Pseudohyphae with budding noted with GMS staining of BAL (400X).

any bacterial growth. Acute hypoxic respiratory failure occurred, and subsequently, endotracheal intubation was performed with mechanical ventilator (MV) support. The CXR revealed poor oxygenation with a bilateral increase in the alveolar process. Bedside cardiac echography showed preserved left ventricular systolic function. Acute respiratory distress syndrome was diagnosed based on the patients' low arterial partial pressure of oxygen ( $\text{PaO}_2$ )/fraction of inspired oxygen ( $\text{FiO}_2$ ) (P/F) ratio. Methylprednisolone at a daily dosage of 1.63 mg/kg and the antibiotic meropenem were prescribed. However, desaturation was still observed with MV support and right lower lung consolidation still progressed. To find evidence of pathogens, BAL was performed, and revealed a yellowish secretion especially in the RUL. Gram staining detected yeast and polymorphonuclear neutrophils (PMN). Both bacterial culture and acid fast staining of the BAL fluid yielded negative results. Cytological analysis of the BAL fluid showed negative findings for malignant cells, but Gomori methenamine silver (GMS) staining revealed numerous PMN and budding pseudo-

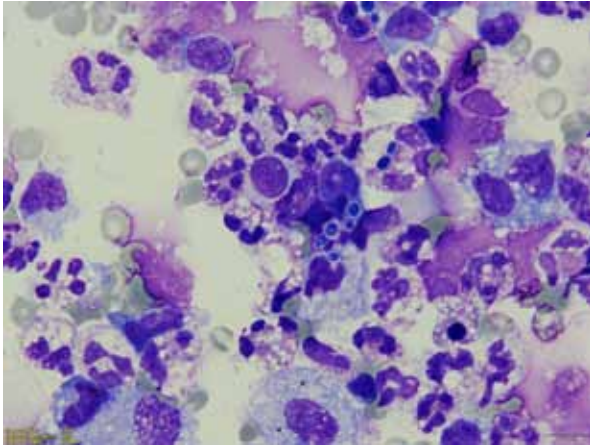


**Fig. 3.** *Candida* spore phagocytosis by neutrophils were noted with Liu's stain in BAL (1000X).

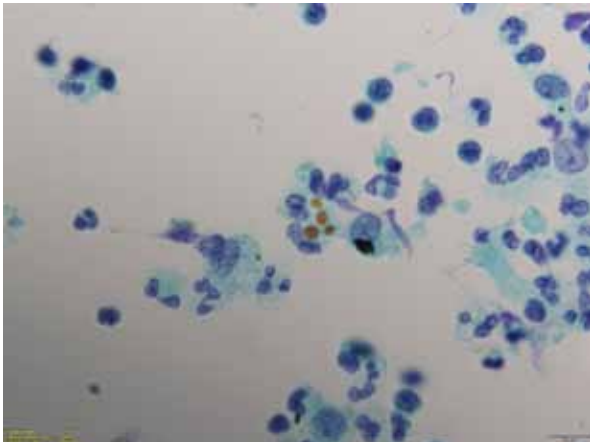


**Fig. 4.** *Candida* spore phagocytosis by neutrophils were noted with Pap's stain of BAL (1000X).

hyphae (Figure 2). Phagocytosis was observed in about 2% of the neutrophils, with intracellular microorganisms visible with Papanicolaou stain (Pap stain) (Figure 3) and Liu's stain (Figure 4). An etiological survey was performed to determine the patient's immunocompromised status, and yielded negative findings for human immunodeficiency virus infection. Finally, the fungal culture of BAL fluid yielded *Candida albicans* with 2,500 colony-forming units (CFU)/ml. The fungal culture from endobronchial

suction also yielded *Candida albicans* about 5 days later. Cultures were negative for *Nocardia* and *Actinomyces*. *Candida* infection was suspected based on the cytological findings, so fluconazole was prescribed. Steroid with methylprednisolone was tapered down and then discontinued due to suspected invasive fungal pneumonia. Methylprednisolone was switched to hydrocortisone for septic shock. However, desaturation was still observed even under high positive end expiratory pressure, along with paralysis by cisatracurium and midazolam due to patient-ventilator dyssynchrony. Chest computed tomography (CT) with contrast was performed again to exclude pulmonary embolism, and revealed progressive changes in the right lung consolidation and abscess formation. In addition, bilateral pleural effusion and left lower lung consolidation was found without any evidence of pulmonary embolism. The *Aspergillus* galactomannan antigen index in the BAL fluid showed a mild elevation of up to 3.17, but was within the normal range in the serum sample. All the fungal cultures from endotracheal tube sputum aspiration showed *Candida albicans*, except 1 sample that showed *Candida albicans* and *Aspergillus niger*. The antifungal agent was then switched to caspofungin after fluconazole use for 1 week to cover a possible *Aspergillus* infection. However, the desaturation status still did not improve, even at 100% FiO<sub>2</sub>, and the patient displayed unstable vital signs. Ultimately, he died due to persistent desaturation and septic shock.

## Discussion

Fungal pneumonia is rare, although it is more frequently observed in patients with hematological diseases and those that are im-

munocompromised. *Candida* pneumonia is an opportunistic fungal infection that is often caused by a congenital or acquired defect in the host immune defenses. A CT-guided or bronchoscopic biopsy should be performed for those patients with indolent lung lesions. BAL is typically not a standard procedure for detecting lung abscess or fungal pneumonia, except *Pneumocystis jirovecii* pneumonia. However, in this particular case, percutaneous lung biopsy and bronchoscopic biopsy were extremely risky because of the patient's acute respiratory failure status and use of MV. The BAL beta-D-glucan test has good sensitivity but inferior specificity for invasive fungal infections [2]. Few case reports of fungal pneumonia in immunocompetent people have been noted in past years. A case report of a 72-year-old male patient with *Candida glabrata* (*C. glabrata*) and *Candida tropicalis* (*C. tropicalis*) pneumonia showed a history of travelling to Ecuador and being exposed to guinea pigs. Fungemia with *C. glabrata* was noted. Both *C. glabrata* and *C. tropicalis* were also found in the BAL fluid specimen [3]. Another case report involved an 83-year-old non-immunosuppressed woman with invasive fatal *Candida* pneumonia. The etiology was probably related to aspiration. At autopsy, she was diagnosed with *Candida* pneumonia [4]. In our case, lung biopsy under poor oxygenation conditions and unstable hemodynamic status was not appropriate. Although a final diagnosis of *Candida* pneumonia requires histopathological evidence of invasive disease, isolating *Candida* from a BAL specimen also confirms the disease [5]. BAL can be performed easily and quickly at the patient's bedside in intensive care while being closely monitored. In addition, cytological evidence with phagocytosis and special stains that define pathogens, especially GMS

stain, can reveal invasive fungal infection. This is considered a good method for diagnosing invasive fungal pneumonia. Moreover, intracellular microorganisms can be detected by Pap stain. Diagnosis of invasive fungal pneumonia by fungal culture from BAL fluid often delays the timing of diagnosis and treatment.

Our patient's condition suddenly deteriorated within 2 to 3 days after we discontinued methylprednisolone and switched to hydrocortisone because of septic shock. We tapered the use of the steroid because we suspected fungal pneumonia. After reviewing the entire course of the disease, we suspected an immune reconstitution inflammatory syndrome (IRIS)-related condition. A few case reports have shown that IRIS occurs only in immunocompromised patients with disseminated candidiasis, Cryptococcus, or mycobacteria infection [6].

There are 2 forms of *Candida* pneumonia. Hematogenously disseminated candidiasis that produces pulmonary lesions is common, whereas primary *Candida* pneumonia due to aspiration of oropharyngeal material is rare [7]. Our patient was associated with the latter etiology because the blood culture did not show any evidence of extrapulmonary organ involvement. The *Candida* species invades by colonization of the airways. However, current Infectious Diseases Society of America guidelines for empirical treatment of invasive *Candida* infection recommend that the preferred empiric therapy for suspected candidiasis in non-neutropenic patients in the ICU is an echinocandin [8]. Fluconazole is an acceptable alternative in patients with no recent azole exposure and no colonization of azole-resistant *Candida* species. Amphotericin B is also an acceptable alternative in patients who are not tolerant to other antifungal agents [8]. Thus, using echinocandins was the

best choice for our patient.

The BAL examination revealed a cut-off value of more than 2% ICO, and the BAL culture yielded more than  $10^4$  colony-forming units (CFU)/mL, which is considered proof of a bacterial infection [1]. Another prospective study revealed that PMNs with ICOs (PIC)  $>1.5\%$  were indicative of ventilator-associated pneumonia [9]. Tracing back to the previous fungal pneumonia or fungal abscess report, fluid retrieved from BAL was used to confirm fungal pneumonia. The percentage of intracellular microorganisms in the BAL fluid showed no cut-off value for the diagnosis of fungal pneumonia. An animal study revealed that BAL-positive ICOs were more accurate than a culture for the diagnosis of recent pneumonia and were less affected by antibiotic treatment [10]. If these rules were applicable to humans, ICOs would be more accurate than a culture via an upper airway aspiration (even including fluid retrieved from BAL) for diagnosis of fungal pneumonia.

Lobar pneumonia with or without cavitation that responds poorly to broad-spectrum antibiotics should indicate the possibility of fungal pneumonia. Percutaneous lung biopsy or transbronchial lung biopsy are extremely risky procedures in patients with endotracheal tube intubation and MV support. BAL with a cytological examination for PIC survey should be performed, particularly in cases with suspected fungal pneumonia and pneumonia with delayed resolution.

## References

1. Ronny MS, Catharina FL, Nele G, *et al.* *Candida* pneumonia in intensive care unit? Open Forum Infect Dis. DOI: 10.1093/ofid/ofu026.
2. Stacey RR, Saraschandra V, Miguel GV, *et al.* The utility of bronchoalveolar lavage beta-D-glucan testing for the diagnosis of invasive fungal infections. *J Infect* 2014; 69: 278-83.
3. Leslie AH, Nicholas RL, Michael RC, *et al.* *Candida glabrata* and *Candida tropicalis* in an immunocompetent patient: a case report. *J Pharm Prac* 2015; 28(3): 284-7.
4. Worthington M. Fatal candidemia pneumonia in a nonimmunosuppressed host. *J Infect* 1983; 7(2): 159-61.
5. Parisa B, Zahra H. Opportunistic invasive fungal infections: diagnosis & clinical management. *Indian J Med Res* 2014 Feb; 139(2): 195-204.
6. Chad JA, Robert DH, Shireesha D, *et al.* Paradoxical immune reconstitution inflammatory syndrome in HIV-infected patients treated with combination antiretroviral therapy after AIDS-defining opportunistic infection. *Clin Infect Dis* 2012; 54(3): 424-33.
7. Ankur G, Dipankar MB, Pavitra MD, *et al.* *Candida* lung abscesses in a renal transplant recipient. *Saudi J Kidney Dis Transpl* 2013; 24(2): 315-7.
8. Peter GP, Carol AK, David RA, *et al.* Clinical practice guideline for the management of candidiasis: 2016 update by the Infectious Diseases Society of America. *Clin Infect Dis* 2016; 62(4): e1-50.
9. Liu C, Du Z, Zhou Q, *et al.* Microscopic examination of intracellular organisms in bronchoalveolar lavage fluid for the diagnosis of ventilator-associated pneumonia: a prospective multi-center study. *Chin Med J* 2014; 127(10): 1808-13.
10. Nilton B, Lucas M, Frederico M, *et al.* Direct examination and cultures of bronchoalveolar lavage in pneumonia diagnosis: a comparative experimental study. *Intensive Care Med* 2007; 33: 1840-7.

## 透過肺泡灌洗術診斷念珠菌肺炎一病例報告

洪緯欣 陽光耀<sup>\*,\*\*</sup>

真菌性肺炎在免疫力正常的病人很難診斷。本病人為一無免疫功能低下危險因子的老年男性，用支氣管沖洗術診斷真菌肺炎。細胞學可發現多型嗜中性白血球中細胞內微生物的比例大於2%，真菌培養最後顯示為白色念珠菌感染，沒有培養出其他細菌。抗黴菌藥物使用之後，此病人最後仍因急性呼吸窘迫徵候群和嚴重敗血症而死亡。( *胸腔醫學* 2017; 32: 266-271)

關鍵詞：念珠菌肺炎，真菌肺炎，支氣管肺泡灌洗術，白血球吞噬作用，細胞內微生物

## IgG4-Related Disease with Pleural Involvement Presenting as Progressive Dyspnea

Pei-Yu Lin, Shih-Chi Ku

Immunoglobulin G4 (IgG4)-related disease is a recognized fibroinflammatory condition. In its pathology, we can see lymphoplasmacytic infiltration, storiform fibrosis and IgG4-positive plasma cells. The disease can involve multiple organ systems, including the lung. In this article, we reported the case of a patient with an initial presentation of hydronephrosis and retroperitoneal mass. The computed tomography-guided biopsy revealed IgG4-related disease. The patient then began to receive weekly dexamethasone treatment (4 mg/week). The mass size decreased gradually, with the disease stabilizing during follow-up. However, a new onset of left pleural effusion developed after 7 years of a stable condition. The pleural fluid analysis revealed lymphocyte-predominant exudate, and the pleural biopsy showed clustered plasma cells and lymphocytes. These plasma cells were mostly IgG4-positive (more than 50 per high-power field). The serum IgG4 level also elevated to 2,490 mg/dL. IgG4-related disease with pleural involvement was diagnosed. The pleural effusion almost totally subsided 1 month after increasing the dose of Predonine to 15 mg/day. (*Thorac Med* 2017; 32: 272-278)

Key words: IgG4-related disease, retroperitoneal mass, pleural effusion

### Introduction

Immunoglobulin G4 (IgG4)-related disease is recognized as a chronic fibroinflammatory disorder [1]. It is characterized by organ swelling with fibrosis and lymphoplasmacytic infiltration, mainly IgG4-positive plasma cells [1-2]. The serum IgG4 level may also be elevated. IgG4-related disease has been reported in several organ systems, including the thyroid, salivary gland, lung, pancreas, kidney, lymph node and large vessel. It is hard to differentiate

IgG4-related disease from malignancy or other diseases with similar presentations. In the respiratory system, the disease can involve the lung parenchyma or pleura, or both. On computed tomography (CT) scanning, 4 main patterns may be seen: a solid nodule, a round-shaped ground glass opacity (GGO), and alveolar interstitial and bronchovascular bundle thickening [4-5]. In affected pleura, we may see pleural thickening or pleural effusion. IgG4-related lung disease is rare. However, IgG4-related disease with pleural involvement is even less

---

Division of Chest Medicine, Department of Internal Medicine, National Taiwan University Hospital, Taipei, Taiwan  
Address reprint requests to: Dr. Shih-Chi Ku, Department of Internal Medicine, National Taiwan University Hospital, College of Medicine, National Taiwan University, No. 7 Chung-Shan South Road, Taipei, Taiwan, 100

described, and rarer when pleural effusion is the sole presentation. We report a case of relapsed IgG4-related disease with dyspnea and pleural effusion.

## Case Report

An 82-year-old male was in a healthy status except for cholecystitis in 2000. He had no underlying illness such as hypertension, diabetes or autoimmune diseases. He began to have lower abdomen discomfort and urinary frequency in June, 2006. The abdomen sonography showed bilateral hydronephrosis. He was then hospitalized in the urology ward for ureterorenoscopy examination. Bladder neck contracture and bilateral dilated pelvis were noted. He then received a transurethral incision of the bladder neck and a bilateral double-J stent insertion. The abdomen and pelvis CT revealed markedly well-enhanced soft tissue tumors at the bilateral renal hila, iliac chain, pelvic sidewall, presacral region and bilateral seminal vesicles. The bilateral renal pelvis was also compressed by these tumors. The CT-guided biopsy (1 November 2006) of the pelvic tumor revealed atypical lymphoid infiltrates. Bone marrow biopsy (13 December 2006) revealed no evidence of lymphoma involvement. The laboratory data showed mild anemia (hemoglobin: 12.3 g/dl) and albumin-globulin reverse (A-G reverse) (albumin: 4.0 g/dL, globulin: 6.1 g/dl). The lactic dehydrogenase, calcium and beta-2 microglobulin ( $\beta$ 2-M) levels were all within a normal range. Serum electrophoresis revealed marked polyclonal gammopathy with increased immunoglobulin G (IgG). Serum immunofixation electrophoresis showed a thin band of IgG/lambda monoclonal gammopathy superimposed on a background of polyclonal gammopathy.

Initial IgG level was 4,390 mg/dl (700-1,600 mg/dl). During hematology outpatient follow-up, repeated CT-guided biopsies of the pelvic tumor still showed atypical lymphocyte infiltrates. The serum IgG level elevated to 5,770 mg/dl, and the IgG4 level was 908 mg/dl (2.4-120 mg/dl). Due to a high degree of suspicion of IgG4-related disease, the patient started to receive weekly glucocorticoid treatment (oral form dexamethasone 4 mg/week) beginning in June, 2007. The abdominal tumors shrank gradually, and the disease status was stable during regular CT follow-ups. The dosage of steroid did not change until dyspnea and left pleural effusion developed in February 2014 (Figure 1A). The chest CT images did not show specific lung parenchymal change or pleural thickening. The abdominal and pelvic tumors remained stationary. Pleural fluid analysis showed lymphocyte-predominant exudates. The cytology and microbiology studies revealed negative results. Overall, the examination did not suggest a specific disease. Pleural biopsy through chest sonography showed clustered plasma cells and lymphocytes, but without significant storiform fibrosis or obliterative phlebitis (Figure 2A-B). The IgG4 immunohistochemical stain showed most plasma cells were IgG4-positive (more than 50 cells under a high-power field) (Figure 2C-D). The serum IgG4 level was elevated to 2,490 mg/dL. Disease progression was favored. We adjusted the glucocorticoid therapy to Predonine 15 mg/day beginning in June, 2014. After treatment for 1 months, the dyspnea improved and the pleural effusion nearly totally disappeared (Figure 1B).

## Discussion

We report the case of a man with IgG4-

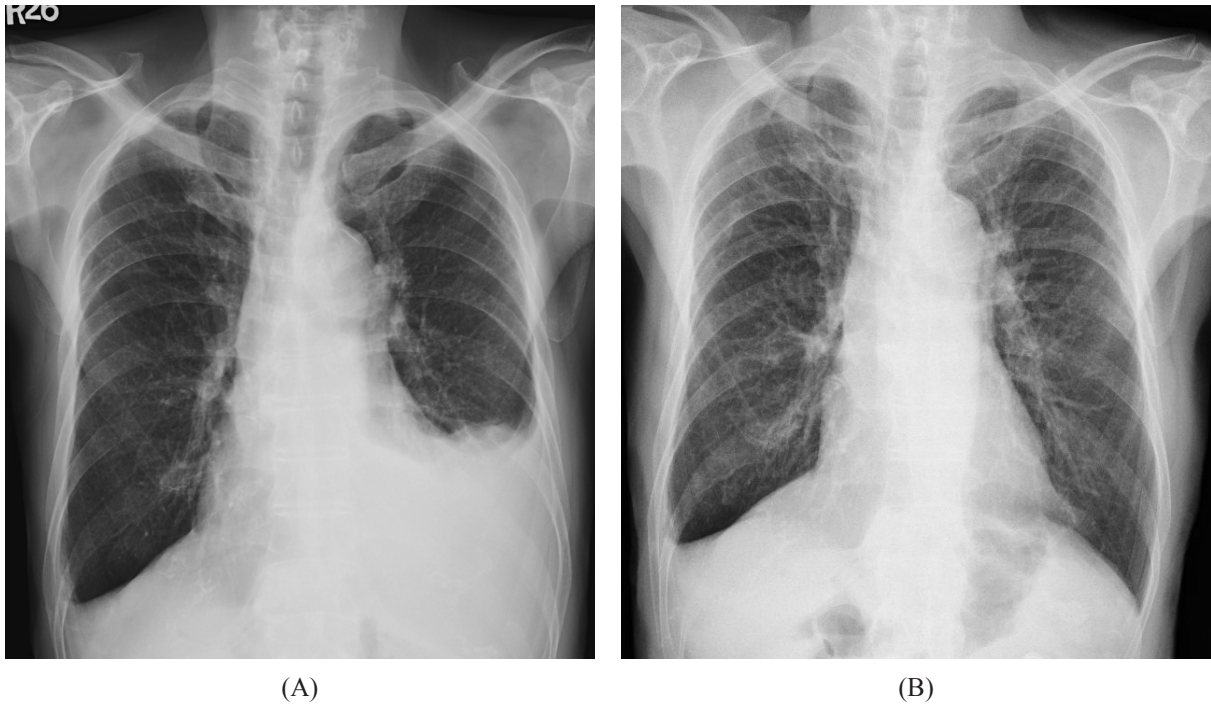


**Fig. 1.** Posterior-anterior (PA) view of chest X-ray. (A) Before adjusting the corticosteroid dosage, the imaging showed right costophrenic (CP) angle blunting and left pleural effusion. (B) After 1 month of Predonine (15 mg/day) treatment. Left pleural effusion was nearly totally subsided.

related disease with an abdominal mass lesion who initially developed dyspnea and a new onset of pleural effusion. IgG4-related disease is a recognized fibroinflammatory condition with tumefactive lesions, a dense lymphoplasmacytic infiltrate rich in IgG4-positive plasma cells, and storiform fibrosis [1-2]. The epidemiology of IgG4-related disease is hard to ascertain because of the low level of awareness of the disease, the diagnostic difficulty, and its various clinical manifestations. The annual incidence of autoimmune pancreatitis (AIP) in Japan in 2001 was estimated to be 1.4 cases per 100,000 people. It is a relatively rare disease and mainly affects older males [3].

To diagnose IgG4-related disease or even to differentiate the disease from other disorders with a similar appearance is difficult. In the

past, there were reports that patients with IgG4-related disease were mistaken as having malignancy and underwent unnecessary surgery. There have been diagnostic criteria for specific organ diseases, such as sialadenitis, dacryoadenitis, IgG4-related pancreatitis and sclerosing cholangitis [6]. The diagnosis of IgG4-related disease is based on a combination of characteristic radiological findings, histopathological findings of abundant lymphocytes and IgG4-positive plasma cells infiltration, storiform fibrosis and obliterative phlebitis, and an elevated IgG4 level ( $\geq 135$  mg/dl) [6-7]. Infiltration of IgG4-positive plasma cells requires an IgG4-positive/IgG-positive ratio  $>40\%$  or  $>10$  IgG4-positive plasma cells under a high-power field [7]. The majority of patients have good glucocorticoid responsiveness. A steroid trial is

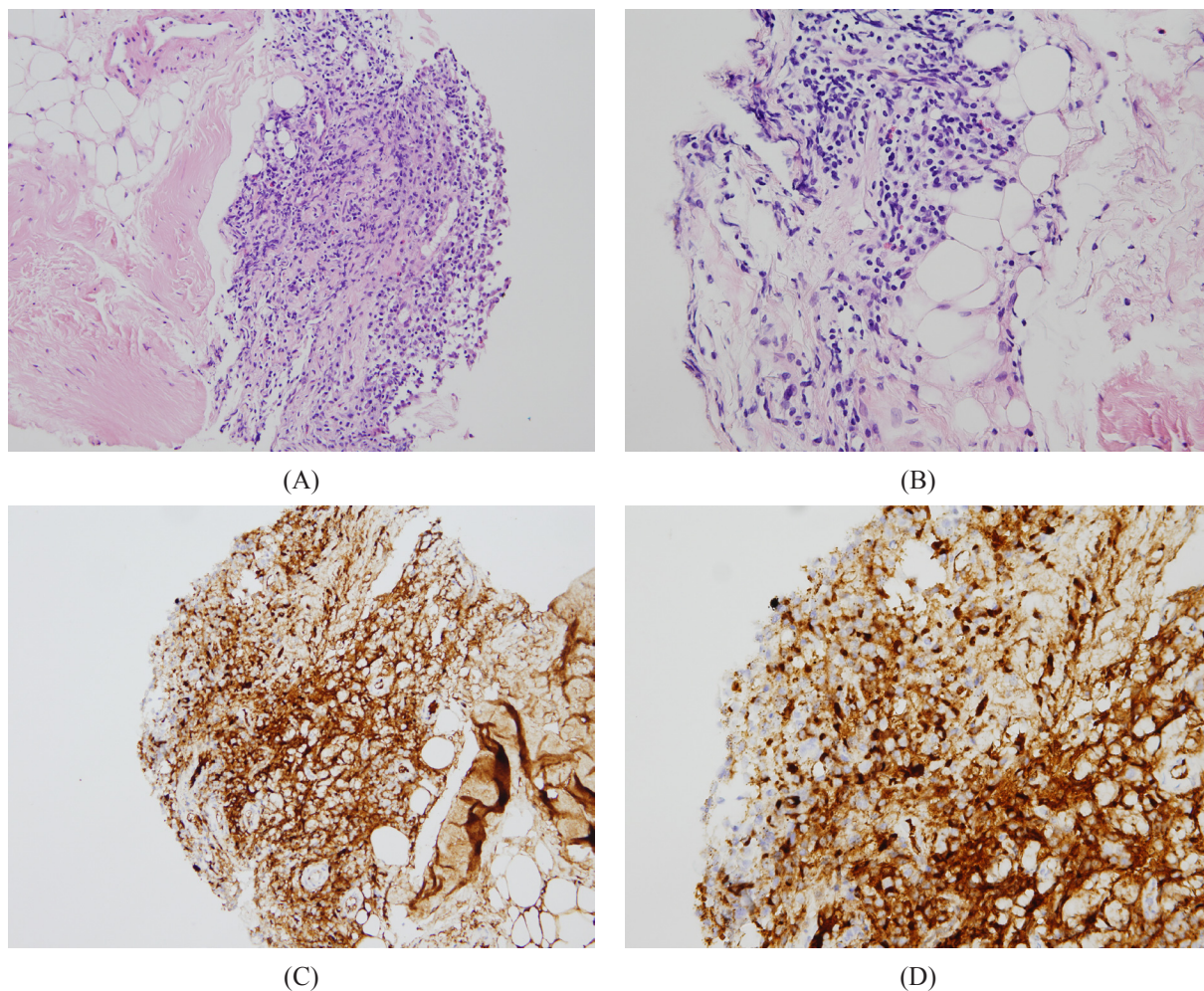


**Fig. 2.** Histologic findings of IgG4-related pleural disease. (A) The pleura showed clustered plasma cells and lymphocytes. No storiform fibrosis or obliterative phlebitis was noted. (hematoxylin-eosin stain, original magnification, x200) (B) Inflammatory cells mainly consisting of lymphocytes and plasma cells. (hematoxylin-eosin stain, original magnification, x400) (C,D) Immunostaining of IgG4 revealed numerous IgG4-positive plasma cells (more than 50 cells per high-power field) (magnification in C, x200; and in D, x400.)

thus seen to be helpful in the diagnosis, but we should carefully rule out malignancy or other illness with a fair steroid treatment response. However, there are indeed some exceptions to the diagnostic criteria. For example, storiform fibrosis is seldom found in affected lymph nodes, and around 30-40% of patients have an IgG4 level in a normal range [4-5]. Also, the histopathology may vary at different stages of the disease, such as the predominantly fibrotic

change in the last stage [2,4-5].

Confirmation of the diagnosis requires adequate time for monitoring and study, and most important, sufficient clinical experience. According to the comprehensive diagnostic criteria of Umehara *et al.* in 2012 [6], our case was classified as “possible” IgG4-related disease in the beginning. We tried glucocorticoid therapy and the response was good. During follow-up, we still arranged regular blood testing and CT

scans to monitor the disease condition. The patient was determined to have “definite” IgG4-related disease after the pleural biopsy. Our patient had no pleural nodule or thickening on either the sonography or the CT, but a pleural biopsy brought out the etiology. It seems to us that IgG4-related disease may possibly affect the pleura before we are able to notice it on current imaging modalities. Likewise, there is a good chance that the lung parenchyma is already affected by the disease. Although we did not perform a lung biopsy, for the next step, we should emphasize the associated changes.

There are still no international guidelines on the management and treatment of IgG4-related disease. Current consensus among experts suggests glucocorticoids for first-line therapy; steroid-sparing immunosuppressive agents such as azathioprine, mycophenolate, and methotrexate for second-line therapy; and rituximab (a monoclonal antibody to B lymphocyte-specific antigen CD20) for third-line therapy [8-9]. Majority of patients with IgG4-related disease respond to glucocorticoids within a few weeks, but some take months and some simply respond poorly. The duration and dosage are based on disease activity. The Japanese consensus guidelines for autoimmune pancreatitis (AIP) suggests prednisolone, a glucocorticoid, at an initial dosage of 0.6 mg/kg/day for 2 to 4 weeks, adjusted to 5 mg/day every 1 to 2 weeks based on clinical presentations, imaging and serology [8,10]. The recommended maintenance dose is 2.5 to 5 mg/day, with effort to discontinue within 3 years depending on clinical improvement. In patients with a poor response or relapse after discontinuing the steroid, an increased dosage or readministration is also suggested [8,10].

Several studies have reported a lower relapse rate in patients with maintenance steroid

therapy than in patients without it. Kamisawa *et al.* reported a 24% relapse rate in 417 AIP patients who received steroid [7]. The relapse rate in patients receiving maintenance therapy was 23%, and in patients discontinuing maintenance therapy, the relapse rate was 34% ( $p < 0.05$ ) [7]. These findings tell us the importance of maintenance therapy, and that single therapy with glucocorticoids will eventually fail to control the disease. In patients who cannot tolerate long-term glucocorticoid or who have poor drug responsiveness, second-line steroid-sparing immunosuppressive agents are thus recommended as single or combination treatment. Rituximab is often reserved for patients who are refractory to steroids and various second-line agents [8,10].

In our case, we gave the patient oral dexamethasone with an initial dosage of 4 mg/week, beginning in June 2007. We chose dexamethasone rather than prednisolone mainly because of uncertainty about the diagnosis at the beginning of the disease course. We gave the patient a relatively lower dosage to monitor clinical improvement. Drug compliance and side effects in the elderly are also considerations. Dexamethasone is a long-acting glucocorticoid with a very strong anti-inflammatory effect. With this treatment, the patient's abdominal discomfort improved and the mass lesion shrank. We then maintained the dexamethasone dosage. After confirmation of IgG4-related disease with pleural involvement, we adjusted the treatment to Predonine 15 mg/day for 1 month, beginning in June 2014. Follow-up chest X-ray at this time showed nearly total resolution of the left pleural effusion. We then tapered Predonine to 10 mg/day for 1 month followed by 5 mg/day up to the present time. There has been no recurrent pleural effusion during follow-up. There have

been several studies on predictive factors for relapse of IgG4-related disease. Initial high IgG4 level, disease with multiple-organ involvement, and male and young at diagnosis have all been reported. However, in our case, there were no similar factors [11].

Several IgG4-related pulmonary diseases have been described in the past. Patients with the disease may present with cough, dyspnea, chest tightness or chest pain, but mostly with non-specific symptoms. The disease can affect the lung parenchyma, interstitium, airways, and pleura. There are 4 characteristic findings of IgG4-related pulmonary disease on CT scanning: a solid nodule (or mass lesion), round-shaped GGO, alveolar interstitial-type findings (honeycombing, bronchiectasis and diffuse GGOs), and bronchovascular-type findings (bronchovascular bundles and interlobular septa thickening) [2,4-5]. Most patients have more than 1 radiologic finding. In affected pleura, we may notice pleural nodules, pleural thickening or pleural effusion. Most patients with affected pleura often have a lung abnormality of the disease. In our case, the patient presented pleural effusion as a sole manifestation. There is no previous data on the prevalence of this kind of manifestation. Over the past few decades, there have been very few case reports of pleural effusion as a sole manifestation. Despite its rarity, we still suggest pleural histopathology for patients with IgG4-related disease with pleural effusion.

## References

1. Terumi K, Kazuichi O. Diagnosis and treatment of IgG4-related disease. *Curr Topics in Microbiol and Immunol* 2017; 401: 19-33.
2. Zen Y, Nakanuma Y. Pathogenesis of IgG4-related disease. *Curr Opin Rheumatol* 2011; 23: 114.
3. Kanno A, Masamune A, Okazaki K, *et al.* Nationwide epidemiological survey of autoimmune pancreatitis in Japan in 2011. *Pancreas* 44(4): 535-9.
4. Zen Y, Inoue D, Kitao A, *et al.* IgG4-related lung and pleura disease: a clinicopathologic study of 21 cases. *Am J Surg Pathol* 2009; 33: 1450.
5. Inoue D, Zen Y, Abo H, *et al.* Immunoglobulin G4-related lung disease: CT finding with pathologic correlations. *Radiology* 2009; 251: 260.
6. Umehara H, Okazaki K, Masaki Y, *et al.* Comprehensive diagnostic criteria for IgG4-related disease (IgG4-RD). *Mod Rheumatol* 2012; 22: 21-30.
7. Kamisawa T, Okazaki K, Kawa S, *et al.* The Working Committee of the Japan Pancreas Society and the Research Committee for Intractable Pancreatic Disease supported by the Ministry of Health, Labour and Welfare of Japan. Amendment of the Japanese consensus guidelines for autoimmune pancreatitis, 2013 III: treatment and prognosis of autoimmune pancreatitis. *J Gastroenterol* 2014; 49: 961-70.
8. Kamisawa T, Shimosegawa T, Okazaki K, *et al.* Standard steroid treatment for autoimmune pancreatitis. *Gut* 2009; 58: 1504-7.
9. Inoue D, Zen Y, Abo H, *et al.* Immunoglobulin G4-related lung disease: CT findings with pathologic correlations. *Radiology* 2009; 251: 260-70.
10. Campbell SN, Rubio E, Loschner AL. Clinical review of pulmonary manifestations of IgG4-related disease. *Annals ATS* 2014; 11: 1466-75.
11. Yamamoto M, Nojima M, Takahashi H, *et al.* Identification of relapse predictors in IgG4-related disease using multivariate analysis of clinical data at the first visit and initial treatment. *Rheumatology* 2015; 54: 45-9.

## IgG4 相關疾病以肋膜侵犯和呼吸喘表現

林珮瑜 古世基

IgG4 相關疾病的致病機轉雖未完全確定，但目前一致認為它和自體免疫相關，全身的器官都有可能被侵犯，IgG4 相關疾病的肺部病例報告相對較少，並不像其對於胰臟或者唾液腺的案例多。本文我們報告一位八十六歲的男性，一開始以腎水腫、後腹腔腫塊來表現，病人經電腦斷層導引切片證實為 IgG4 相關疾病，血液中 IgG4 數值也上升，腫塊在類固醇治療後逐漸變小，然而卻在治療穩定時，病人出現新的肋膜積液，肋膜積液分析顯示為淋巴球為主的滲出液，其餘細胞學檢查和培養皆為陰性，病人最後接受肋膜切片才發現一樣是 IgG4 相關疾病導致。(胸腔醫學 2017; 32: 272-278)

關鍵詞：IgG4 相關肺部疾病，肋膜積液，肋膜切片

# Endobronchial Ultrasound Imaging of Castleman's Disease: Two Case Reports

Yung-Hsuan Chen, Chao-Chi Ho

Castleman's disease (CD) is a rare lymphoproliferative disorder that usually involves the mediastinum. The diagnosis of CD is usually established by excisional lymph node biopsy. Based on the histological features, the disease can be classified into 3 types: hyaline-vascular, plasma cell type, and mixed type. We report the cases of 2 patients with CD, both of whom underwent endobronchial ultrasound (EBUS) and surgical biopsy. In the first case, EBUS showed a hilar mass with hypervascularity, and the final diagnosis was hyaline-vascular-type CD. In the second case, EBUS showed lymphadenopathy at group 11R with hypovascularity, and the final diagnosis was plasma cell-type CD. For those CD patients with an initial presentation of mediastinal lymphadenopathy, pre-operative EBUS imaging might provide more information on the lesion. Moreover, EBUS-guided transbronchial needle aspiration could even enable sampling of tissue cores for histological diagnosis. (*Thorac Med* 2017; 32: 279-285)

Key words: Castleman's disease, endobronchial ultrasound, hilar mass, mediastinal lymphadenopathy

## Introduction

Castleman's disease (CD) is a rare lymphoproliferative disorder with an unknown etiology; it was first described by Castleman in 1954 [1]. CD usually involves the mediastinum, and could be unicentric or multicentric. Based on the histological features, the disease is classified into 3 types: hyaline-vascular, plasma cell type, and mixed type [2-3]. Diagnosis of CD is usually established by excisional lymph node biopsy, because the normal appearance of cells isolated from the entire lymph node may lead to

a failure to diagnose CD when using fine needle aspiration [4]. However, for those CD patients with an initial presentation of mediastinal lymphadenopathy, pre-operative endobronchial ultrasound (EBUS) imaging might provide more hints of the tentative diagnosis. We report 2 similar cases of CD and their EBUS imaging.

## Case Reports

### Case 1

A 23-year-old woman presented with intermittent chest pain and progressive dyspnea for

---

Division of Pulmonary and Critical Care Medicine, Department of Internal Medicine, National Taiwan University Hospital, Taipei, Taiwan

Address reprint requests to: Dr. Chao-Chi Ho, Division of Pulmonary and Critical Care Medicine, Department of Internal Medicine, National Taiwan University Hospital, Taipei, Taiwan, #7 Chung-Shan South Road, Taipei, Taiwan

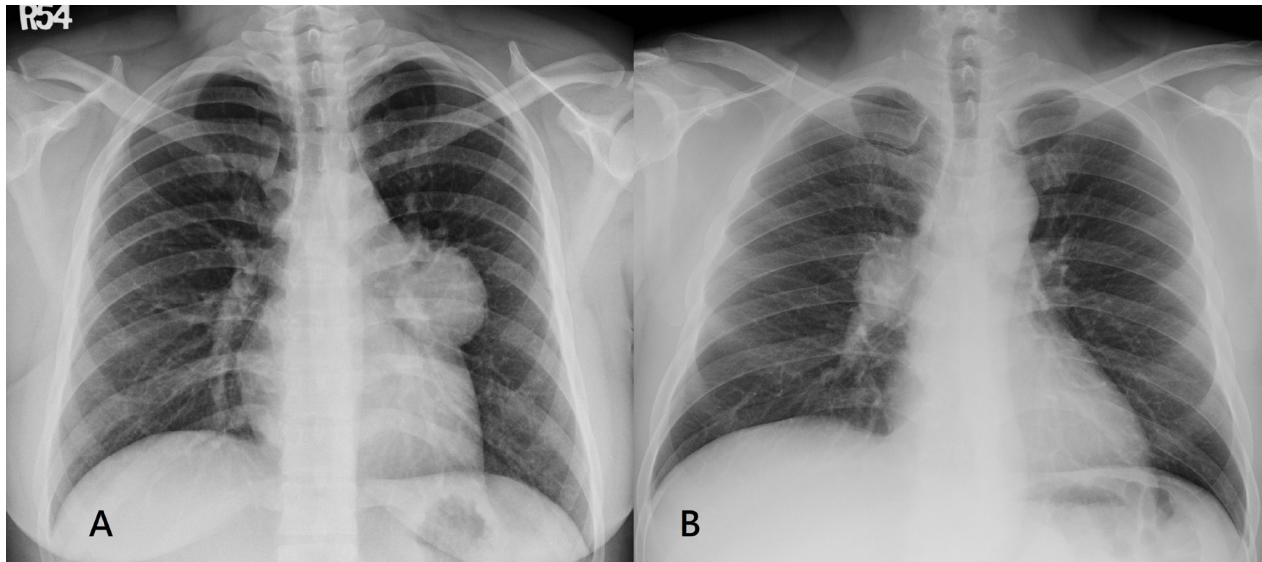


**Fig. 1.** CXR of the 2 cases. A well-circumscribed round mass shadow at the A: left lung hilum (Case 1), and B: right lung hilum (Case 2) is seen on CXR in each case.

1 month. Sporadic hemoptysis was also noted. She denied fever, productive cough, palpitation, or referred pain. Physical and serological examination findings were unremarkable. The electrocardiogram and echocardiogram were normal, but her chest X-ray (CXR) showed a left hilar mass (Figure 1A). The computed tomography (CT) of her chest revealed a large left hilar mass with homogeneous enhancement, 7.3 cm in diameter, which resulted in external compression of segmental bronchi of the left upper lobe (LUL) (Figure 2A). Thoracic magnetic resonance imaging (MRI) also revealed a mass lesion at the left hilum with enhancement and lymphadenopathy at the left mediastinum. The differential diagnosis included lymphoma, CD, and carcinoid tumor. EBUS of the lesion was performed, and revealed a huge homogeneous mass with hypervascularity at the left hilum (Figure 3A). Transbronchial needle aspiration (TBNA) was not performed because of the high bleeding risk.

The patient later underwent thoracotomy

for tumor resection by chest and cardiovascular surgeons. During surgery, a well-defined, encapsulated and hypervascularized tumor, with a maximum diameter of 7 cm, was found at the left hilum (Figure 4). The left pulmonary vein was pushed to the medial site by the tumor and was preserved during the operation. The tumor surface bled easily. Part of the tumor was removed and the deeper part was left in place. Pathology reported a lymph node with subcapsular sinus obliteration and multiple diffuse atrophic follicles, which contained stromal hyalinization, concentric rimming of the mantle zone, and occasional twinning of germinal centers (Figure 5). High endothelial venule proliferation between these atrophic follicles, without prominent plasma cell infiltration or sheet-like growth of follicular dendritic cells, was evident. There was no atypical large plasmablastic cell or positive HHV-8 nuclear staining. The picture was compatible with hyaline-vascular-type CD.

The patient had a smooth postoperative course and started steroid use 1 month after sur-

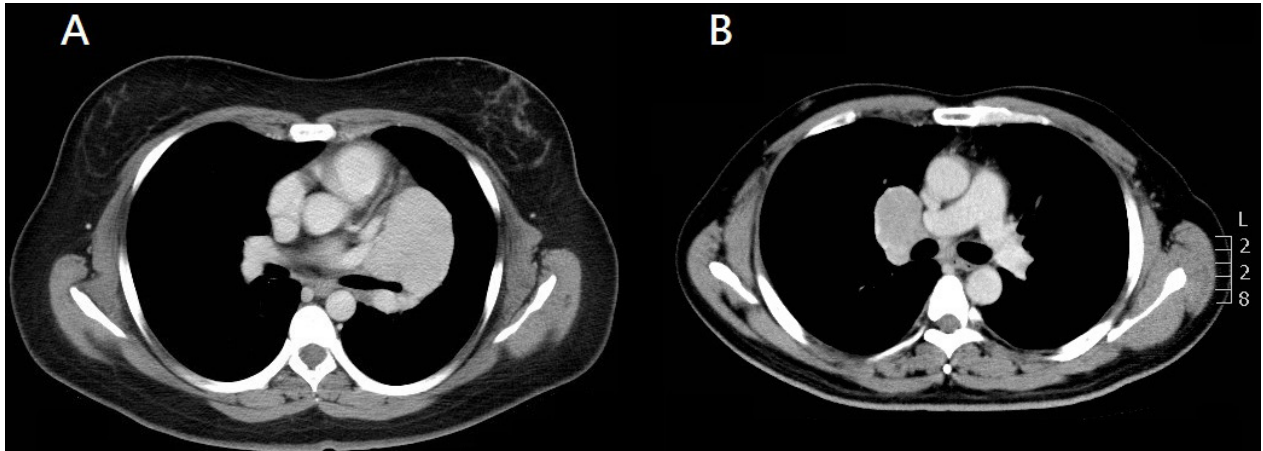


**Fig. 2.** Thoracic CT of the 2 cases. A: Case 1, a large left hilar mass with homogeneous enhancement; B: a soft tissue mass at the right hilum and lymphadenopathy at the subcarina.

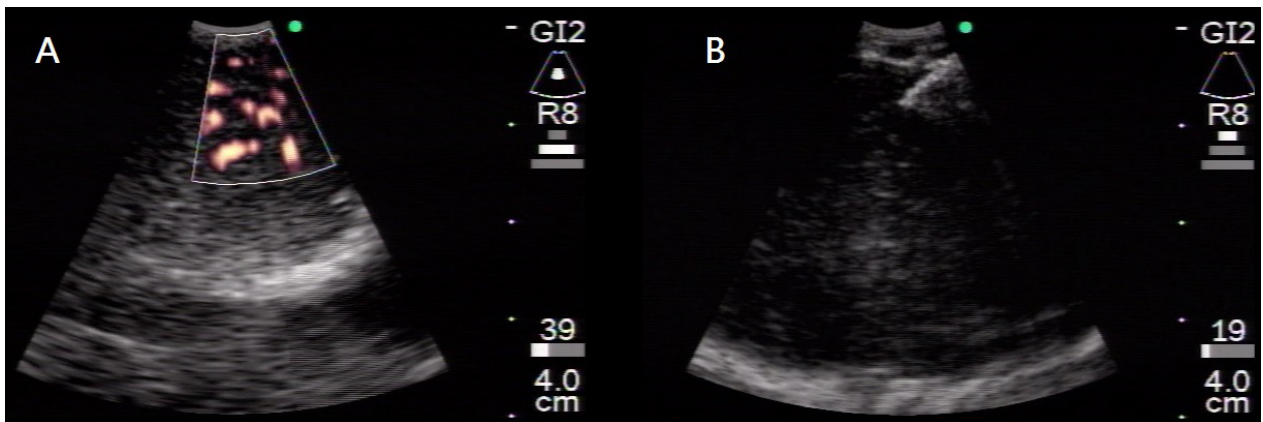


**Fig. 3.** EBUS imaging of the 2 cases. A: Case 1, a huge homogeneous mass with hypervascularity at the left hilum; B: Case 2, EBUS-TBNA of the right hilar tumor shows the needle within the tumor.

gery. About 6 months later, thoracic CT showed a residual tumor with less lymphadenopathy at the left mediastinum.

### Case 2

A 47-year-old man sought a second opinion because of an incidental finding of a right hilar mass on CXR (Figure 1B). Thoracic CT revealed a 5.8 cm soft tissue mass at the right hilum and lymphadenopathy at the pretracheal retrocaval space, subcarina, and anterior medi-

astinum (Figure 2B). There was no discomfort and the serological examination was unremarkable. Whole body positron emission tomography showed probable FDG-avid malignancies at both the right upper lobe region and right lower paratracheal lymph nodes. No abdominal lymphadenopathy was found. The patient underwent EBUS-TBNA to obtain a histological core biopsy specimen. EBUS showed lymphadenopathy at group 11R with heterogeneity and hypovascularity; TBNA was performed

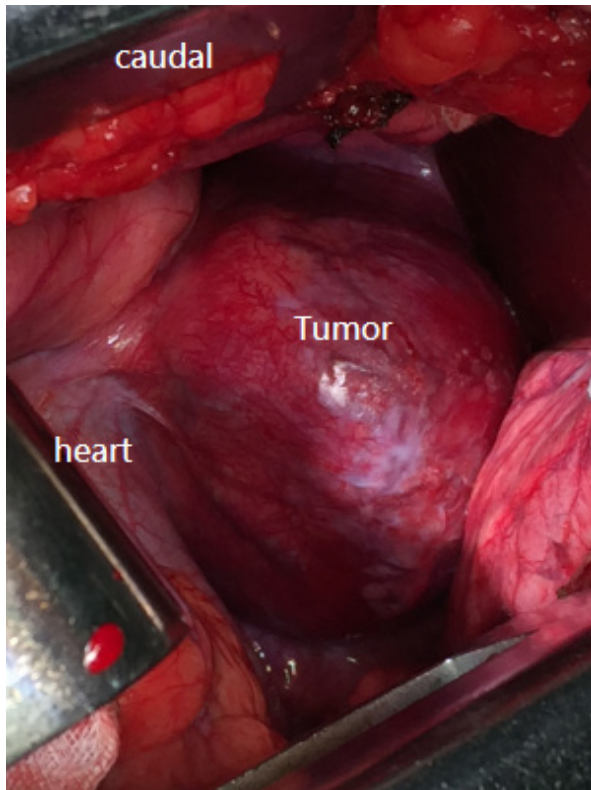


**Fig. 4.** Thoracotomy finding shows a well-defined, encapsulated and hypervascularized tumor, with a maximum diameter of 7 cm at the left hilum.

smoothly with tissue core (Figure 3B). Pathology revealed tiny lymphoid tissue without evidence of malignancy (Figure 5B). No granulomatous inflammation was found.

To obtain a definite diagnosis, biopsy of the mediastinal lymphadenopathy (Groups 3, 4, and 7) via right-side video-assisted thoracoscopy was used. Pathology reported interfollicular plasmacytosis without conspicuous cytological atypia of plasma cells. No vascular proliferation, storiform fibrosis, or obliterative phlebitis was found. The picture was compatible with plasma cell-type CD. Blood immunofixation electrophoresis revealed no monoclonal gammopathy. Based on the above findings, the diagnosis of unicentric plasma cell CD was con-

firmed.

## Discussion

Castleman's disease, alternatively known as angiofollicular lymph node hyperplasia, is a rare lymphoproliferative disorder that was first described by Benjamin Castleman in 1954 [1]. Later, Castleman and colleagues identified a series of patients with solitary hyperplastic mediastinal lymph nodes containing small, hyalinized follicles and a marked interfollicular vascular proliferation (hyaline-vascular-type CD) [5]. In subsequent years, serial case reports revealed another variant of CD, plasma cell type, in which the histology of the patients' lymph nodes showed a germinal center with sheets of plasma cells in the germinal center and in the interfollicular space without vascular proliferation or hyalinization [3]. On the basis of the extent of disease involvement, CD was differentiated into unicentric (UCD) and multicentric (MCD) types. UCD is most commonly the hyaline-vascular type of CD, and MCD is typically the plasma cell type of CD [6].

Hyaline-vascular-type CD accounts for 90% of cases of CD and is unicentric in 90% of cases. It occurs most often in young adults, and is diagnosed at a median in their 3<sup>rd</sup> or 4<sup>th</sup> decade of life. It usually manifests as an asymptomatic mass lesion with a benign course [7]. Treatment includes curative surgical resection for UCD and systemic treatment, such as steroid or chemotherapy, for MCD and aggressive forms [6,8]. In our first case, the patient was diagnosed as having hyaline-vascular-type UCD. Curative resection failed because of the lesion's relationship with the great vessels. She then received oral prednisolone as follow-on treatment. The mediastinal lymphadenopathy and residual hilar

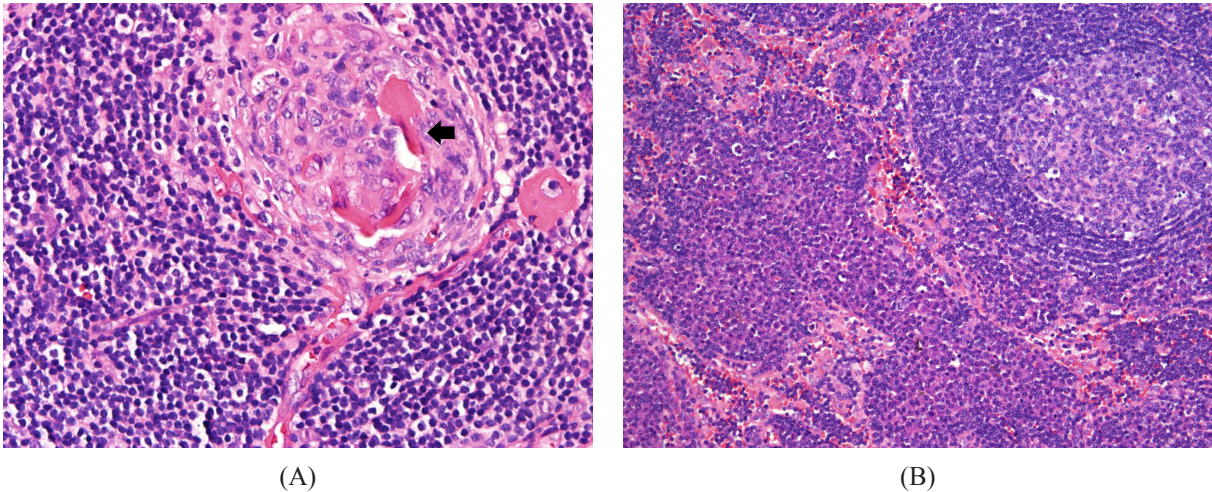


**Fig. 5.** Hematoxylin-eosin stain of the specimens obtained by surgery in the 2 cases. A: Stromal hyalinization within germinal follicles (arrows) without malignant findings (HE,  $\times 400$ ); B: Interfollicular plasmacytosis without conspicuous cytological atypia of plasma cells or vascular proliferation (HE,  $\times 100$ )

mass were reduced in size 6 months later.

Less than 10% of CD cases are plasma cell type. Of these cases, the unicentric form seems to be less common than the multicentric form, although some reported cases of UCD might derive from incompletely documented MCD [6]. Most cases of MCD occur later in life, with a median age in the 6<sup>th</sup> decade. Those patients who have plasma cell-type CD have a greater tendency to experience systemic symptoms and laboratory abnormalities, such as fever, night sweats, malaise, anemia, thrombocytopenia, and hyperglobulinemia. Multifocal lymphadenopathy or hepatosplenomegaly is also found in some cases [3]. Common therapies for plasma cell-type CD include systemic chemotherapy and antiproliferative agents, including anti-interleukin 6 receptor and anti-CD20 antibody treatment [9]. In case 2, lymphadenopathy was found only in the mediastinum in the image study. The patient also had no other systemic manifestation. Systemic treatment had been planned for the patient but he was subsequently

lost to follow-up.

Confirming the diagnosis of CD is usually a challenging process. Most cases require excisional lymph node biopsy to obtain histological evidence. EBUS-TBNA is a real-time procedure for biopsy of mediastinal and hilar lesions, and has become the first choice for staging mediastinal lymphnodes [10]. EBUS-TBNA can be performed using a 22-gauge (G) or 21G dedicated TBNA needle. A single-center study suggested 21G TBNA needles are superior to 22G needles in characterizing benign lesions and non-small cell lung cancer when performing histopathological assessment [11]. The EBUS images of our patients were consistent with their final diagnoses, in that the hyaline-vascular-type CD had a hilar lesion with hyper-vascular echogenicity, while the plasma cell-type CD did not.

In conclusion, for those patients who have an initial presentation of mediastinal lymphadenopathy, pre-operative EBUS imaging might provide more information, and EBUS-TBNA

could even enable sampling of tissue cores for histological diagnosis.

## References

1. Castleman B, Towne VW. Case records of the Massachusetts General Hospital; weekly clinicopathological exercises; founded by Richard C. Cabot. *N Engl J Med* 1954; 251(10): 396-400.
2. Gaba AR, Stein RS, Sweet DL, *et al.* Multicentric giant lymph node hyperplasia. *Am J Clin Pathol* 1978; 69(1): 86-90.
3. Keller AR, Hochholzer L, Castleman B. Hyaline-vascular and plasma-cell types of giant lymph node hyperplasia of the mediastinum and other locations. *Cancer* 1972; 29(3): 670-83.
4. Cangiarella J, Weg N, Symmans WF, *et al.* Aspiration cytology of signet-ring cell lymphoma. A case report. *Acta Cytol* 1997; 41(6): 1828-32.
5. Castleman B, Iverson L, Menendez VP. Localized mediastinal lymphnode hyperplasia resembling thymoma. *Cancer* 1956; 9(4): 822-30.
6. Cronin DM, Warnke RA. Castleman disease: an update on classification and the spectrum of associated lesions. *Adv Anat Pathol* 2009; 16(4): 236-46.
7. Tey HL, Tang MB. A case of paraneoplastic pemphigus associated with Castleman's disease presenting as erosive lichen planus. *Clin Exp Dermatol* 2009; 34(8): e754-6.
8. Ko SF, Hsieh MJ, Ng SH, *et al.* Imaging spectrum of Castleman's disease. *AJR Am J Roentgenol* 2004; 182(3): 769-75.
9. Nicoli P, Familiari U, Bosa M, *et al.* HHV8-positive, HIV-negative multicentric Castleman's disease: early and sustained complete remission with rituximab therapy without reactivation of Kaposi sarcoma. *Int J Hematol* 2009; 90(3): 392-6.
10. Ho CC, Lin CK, Yang CY, *et al.* Current advances of endobronchial ultrasonography in the diagnosis and staging of lung cancer. *J Thorac Dis* 2016; 8(Suppl 9): S690-6.
11. Jeyabalan A, Shelley-Fraser G, Medford AR. Impact of needle gauge on characterization of endobronchial ultrasound-guided transbronchial needle aspiration (EBUS-TBNA) histology samples. *Respirology* 2014; 19(5): 735-9.

## Castleman 氏病的支氣管內視鏡超音波影像－案例報告

陳永瑄 何肇基

Castleman 氏病是一種罕見且經常侵犯縱膈腔的淋巴增生性疾病，其診斷常藉由手術來執行淋巴結切片。此病可依據組織學特色分成以下三種類型：透明血管型、漿細胞型、及混和型。我們提出討論的兩位 Castleman 氏病個案皆有接受支氣管內視鏡超音波檢查及淋巴結切片手術。第一位個案的支氣管內視鏡超音波檢查發現有一富血管性之肺門腫塊，其最後診斷為透明血管型 Castleman 氏病；第二位則是經支氣管內視鏡超音波檢查發現有 HR 的淋巴結腫大且較不具有血管分布，其最後診斷為漿細胞型 Castleman 氏病。術前支氣管內視鏡超音波檢查的影像或許可提供給臨床人員更多關於病灶的資訊。當病灶可執行經支氣管內視鏡超音波指引細針抽吸時，有機會取得足夠的檢體以得到組織學診斷。( *胸腔醫學* 2017; 32: 279-285)

關鍵詞：Castleman 氏病，氣管內視鏡超音波，肺門腫塊，縱膈腔淋巴結腫大

# Special Histological Type of Synchronous Primary Lung Cancer

Hui-Ju Ho\*, Wei-Heng Hung\*\*, Bing-Yen Wang \*\*, \*\*\*, \*\*\*\*

A 62-year-old man visited our outpatient department due to a 2.0-cm pulmonary nodule with irregular margins in the left perihilar region that was found on chest x-ray at another institution; however, the patient had experienced no discomfort. This case was a special histological type of synchronous primary lung cancer with adenosquamous carcinoma at the left lower lobe and mixed small cell carcinoma and squamous cell carcinoma at the right lower lobe. Our experience with this case highlights the importance of distinguishing between multiple primary lung cancer and distant lung metastasis. (*Thorac Med* 2017; 32: 286-290)

Key words: synchronous, lung cancer, small cell carcinoma, squamous cell carcinoma, adenosquamous carcinoma

## Introduction

Distinguishing between synchronous primary lung cancers and multiple metastatic lung cancer is essential and sometimes difficult. Here, we present the case of a 62-year-old man who was diagnosed as having synchronous primary lung cancer with adenosquamous carcinoma at the left lower lobe (LLL) and mixed small cell carcinoma and squamous cell carcinoma (SCC) at the right lower lobe (RLL). This case highlights the importance of distinguishing between multiple primary lung cancer and distant lung metastasis.

## Case Presentation

A 62-year-old man visited our outpatient department because a 2.0-cm nodule with irregular margins in the left perihilar region had been found on chest x-ray at another institution. However, the patient had experienced no discomfort. Chest computed tomography (CT) showed a 4.0-cm nodule at the left lower lobe (Figure 1A), and squamous cell carcinoma was reported on CT-guided biopsy. A 2.0-cm nodule at the right lower lobe (Figure 1B) was also observed on chest CT. No obvious mediastinal lymph node enlargement was observed on the chest CT. Brain magnetic resonance imaging (MRI) and bone scans showed no metastasis.

---

\*Department of surgery, division of thoracic department, EDA cancer hospital; \*\*Division of Thoracic Surgery, Department of Surgery, Changhua Christian Hospital and Institute of Medicine, Taiwan; \*\*\*Division of Thoracic Surgery, Department of Surgery, Taipei Veterans General Hospital and \*\*\*\*National Yang-Ming University School of Medicine, Taipei, Taiwan

Address reprint requests to: Dr. Bing-Yen Wang, Division of Thoracic Surgery, Department of Surgery, Changhua Christian Hospital, No. 135, Nanxiaoou St, Changhua City, Changhua cCounty 500, Taiwan (R.O.C.)

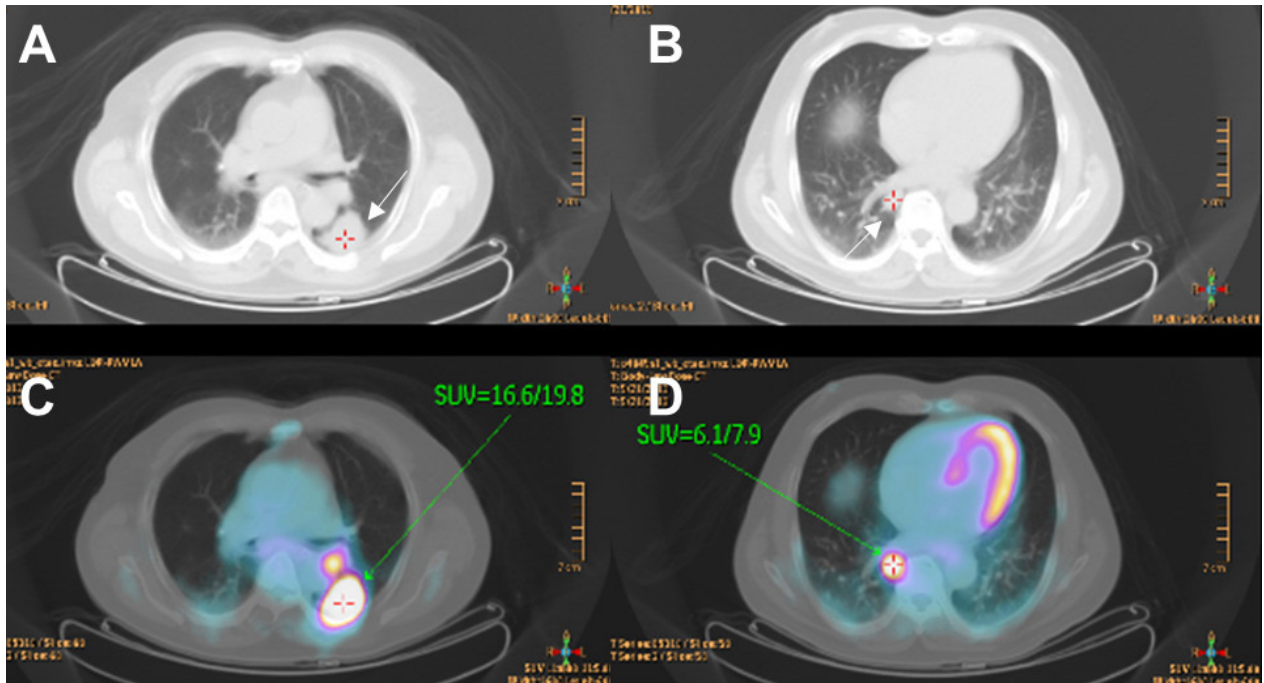


**Fig. 1.** (A and B) Chest computed tomography (CT) findings. (A) A 4.0-cm nodule was observed at the left lower lobe (LLL). (B) A 2.0-cm nodule was observed at the right lower lobe (RLL). (C and D) Positron emission tomography (PET)/CT findings. (C) The LLL showed intensely increased fluorodeoxyglucose (FDG) uptake (early/delayed maximum standardized uptake value [SUVmax] = 16.6/19.8). (D) The RLL also showed intensely increased FDG uptake (early/delayed SUVmax = 6.1/7.9).

Positron emission tomography (PET)/CT scan revealed intensely increased fluorodeoxyglucose (FDG) uptake at the LLL (early/delayed maximum standardized uptake value [SUVmax] = 16.6/19.8; Figure 1C) and RLL (early/delayed SUVmax = 6.1/7.9; Figure 1D). LLL lung cancer with pulmonary tuberculosis or double primary lung cancer was suspected. There was no significant FDG uptake at the mediastinal lymph nodes on the PET/CT.

RLL biopsy was performed and the initial pathology report showed small cell carcinoma in the right lower lung. Synchronous primary lung cancer was diagnosed. Then, thoracoscopic lobectomy of the RLL and radical lymph node dissection were performed, since the central tumor precluded wedge resection. The pathology report showed mixed small cell carcinoma

and SCC (Figure 2A). The hilar, paratracheal, and subcarinal lymph nodes revealed metastatic mixed small cell carcinoma and SCC, but the interlobar lymph node was negative for malignancy. The pathologic stage was classified as pT1bN2M0.

The patient was readmitted for surgical thoracoscopic wedge resection of the LLL and radical lymph node dissection 1 month later, and lobectomy was performed on the right side. The pathology report revealed adenosquamous carcinoma (Figure 2B). The hilar lymph node showed metastatic adenosquamous carcinoma, but the lymph nodes at the aortopulmonary window and inferior pulmonary ligament were negative for malignancy. The pathologic stage was classified as pT2aN1M0. The final diagnosis was synchronous primary lung cancer

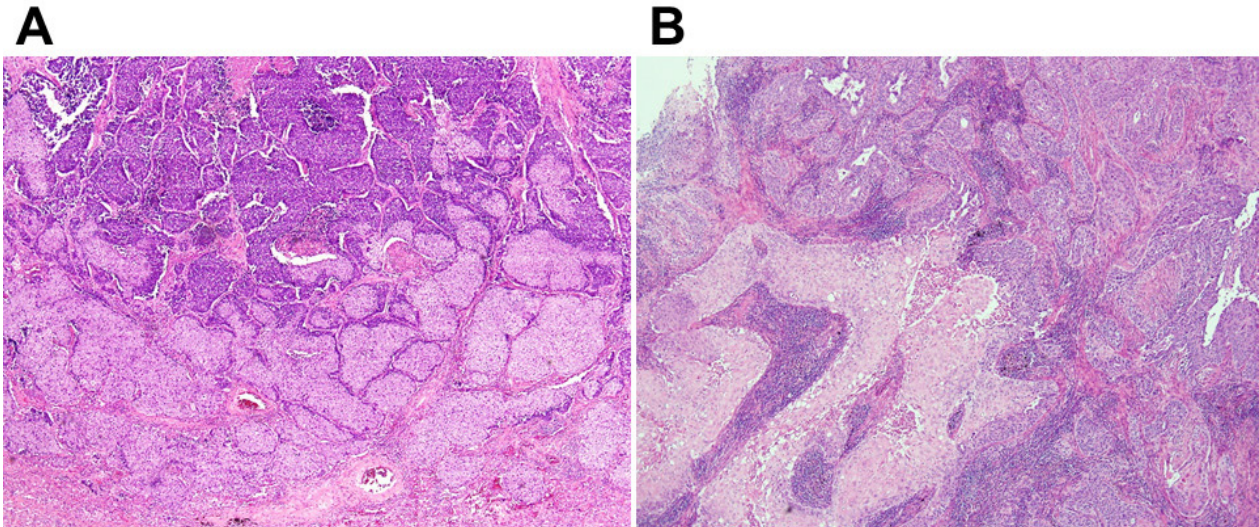


**Fig. 2.** (A) Tumor cells of the right lower lung were arranged in a solid nest pattern with 2 populations: squamous cell carcinoma (SCC) (lower portion) with a pale eosinophilic appearance and small cell carcinoma with hyperchromatic tumor cells and central necrosis (upper portion) (original magnification, 40 $\times$ ). (B) The left lower lung tumor revealed adenosquamous carcinoma composed of SCC with solid nests of keratinized tumor cells (lower left portion) and adenocarcinoma in a glandular to solid pattern (upper portion) (original magnification, 40 $\times$ ).

with mixed small cell carcinoma and squamous cell carcinoma over the right lower lobe, stage pT2aN2M0, and adenosquamous carcinoma over the left lower lobe, stage pT1bN1M0.

Microscopic examination revealed that the right lower lung tumor consisted of 2 tumor populations: SCC and small cell carcinoma. SCC was immunoreactive for p40, but negative for TTF-1, CD56, and synaptophysin. However, the small cell carcinoma area was positively immunoreactive to TTF-1, CD 56, and synaptophysin, and negative for p40. The left lower lung tumor revealed adenosquamous carcinoma composed of SCC with keratinized tumor cells and focal adenocarcinoma with a glandular to solid growth pattern. The SCC area was positively immunoreactive for p40, and the adenocarcinoma area was positively immunoreactive for CEA and mucin stain.

After surgery, the patient was discharged and presented for follow-up at the outpatient

department. Adjuvant chemotherapy with docetaxel (Taxotere) and platinum was prescribed and radiation therapy was also performed.

## Discussion

The concept of multiple primary lung cancer was first described by Beyreuther [1] in 1924, and was classified as either synchronous (more than 1 primary lesion arising in the lung at the same time) or metachronous (developing a second primary lung cancer after treatment of the initial lesion) lung cancer. Since then, numerous studies have been published, and the prevalence of multiple primary lung cancer was estimated at 1-10%. However, no clear definition of multiple primary lung cancer existed until the Martini and Melamed criteria [2] were published in 1975. These criteria are widely used now to diagnose multiple primary lung

cancer worldwide. The criteria for synchronous primary lung cancer, defined as concurrent, separate, malignant lung epithelial neoplasms with different histologies, or tumors of a similar histology arising in different locations (segments, lobes, or lung), include: (1) origin from carcinoma in situ, (2) no carcinoma in the common lymphatics, and (3) no extrapulmonary metastasis at the time of diagnosis.

Using the statistical results of previous studies [3-5], we found that a similar histologic type was more commonly observed than different histologic types in synchronous primary lung cancer. In these studies, adenocarcinoma was the most common histologic type and SCC was the second most prevalent. In different histologic-type synchronous primary lung cancer, adenocarcinoma with SCC was the most common histologic type. Small cell carcinoma, large cell carcinoma, and neuroendocrine carcinoma with other histologic types were also reported, but rarely. Adenosquamous carcinoma was mentioned only in similar histologic-type cancer, and was never reported in mixed histologic-type cancer.

In this article, we described a rare case of different histologic-type synchronous primary lung cancer with a special histologic type, i.e., adenosquamous carcinoma at the LLL and mixed small cell carcinoma and SCC at the RLL. In a review of the literature [3-5], adenosquamous carcinoma was mentioned only in similar histologic-type cancer; mixed small cell carcinoma and SCC was not reported in either similar or different histologic-type cancer.

Due to the spread of lung cancer screening and other advanced diagnostic tools, more lung cancer patients are being diagnosed at an early stage. Therefore, early-stage diagnosis of multiple lung cancer is also increasing. The treat-

ment for multiple primary lung cancer remains controversial, but research on this disease has increased recently. Several studies [3-5] have discussed surgical treatment for multiple primary lung cancer and came to a similar conclusion: that in patients at an early stage, aggressive resection led to a more favorable long-term prognosis and higher survival rate than in patients with distant metastasis (M1) or variants of T4 tumors.

## Conclusion

It is important to aggressively confirm the histologic type in lung cancer patients, particularly in those with multiple lung nodules, in order to avoid misdiagnosis of multiple primary lung cancer. Distinguishing between multiple primary lung cancer and distant metastasis is critical, as surgical outcomes of aggressive resection in multiple primary lung cancer patients are much better than those of patients with distant lung metastasis.

## References

1. Beyreuther H. Multiplicate von carcinomen bei einem fall von sog. Scheneberger Lungenkrebs mit tuberkulose. *Virchows Arc* 1924; 250: 230-43.
2. Martini N, Melamed MR. Multiple primary lung cancers. *J Thorac Cardiovasc Surg* 1975; 70: 606-12.
3. Yu YC, Hsu PK, Yeh YC, *et al.* Surgical results of synchronous multiple primary lung cancers: similar to the stage-matched solitary primary lung cancers? *Ann Thorac Surg* 2013; 96: 1966-74.
4. Reinmuth N, Stumpf A, Stumpf P, *et al.* Characteristics and outcome of patients with second primary lung cancer. *Eur Respir J* 2013; 42: 1668-76.
5. Tanvetyanon T, Finley DJ, Fabian T, *et al.* Prognostic factors for survival after complete resections of synchronous lung cancers in multiple lobes: pooled analysis based on individual patient data. *Ann Oncol* 2013; 24: 889-94.

## 同時性原發性肺癌的特殊病理發現病例報告

何蕙如\* 洪維亨\*\* 王秉彥\*\*,\*\*\*,\*\*\*\*

同時性原發性肺癌的定義須符合：同時發生且為分別獨立的、不同病理型態的惡性肺上皮增生或相同病理型態但在不同區域（對側肺、不同肺或不同肺段）的癌症；另外還同時須符合下列三點：1. 源自原發性肺癌，2. 在共同的淋巴區域沒有惡性細胞，3. 在診斷的同時沒有遠端的轉移。

在這個病例報告我們提出了一位在左側肺門有兩公分的肺結節而沒有任何臨床症狀的62歲男性，在最終的手術取得標本確認為左下肺葉腺鱗狀細胞癌及右下肺葉混合小細胞及鱗狀細胞癌，在此報導中則凸顯出分辨不同的病理細胞型態對於診斷原發性或轉移性肺癌的重要性。（*胸腔醫學* 2017; 32: 286-290）

關鍵詞：同時性原發性肺癌，小細胞癌，鱗狀細胞癌，腺鱗狀細胞癌

---

\* 義大癌治療醫院 胸腔外科，\*\* 彰化基督教醫院 胸腔外科，\*\*\* 台北榮民總醫院 胸腔外科，\*\*\*\* 國立陽明大學  
索取抽印本請聯絡：王秉彥醫師，彰化基督教醫院 胸腔外科，500 彰化市南校街 135 號